

1 **Basin-scale multi-objective simulation-optimization modeling for**  
2 **conjunctive use of surface water and groundwater in northwest China**

3 Jian Song<sup>a</sup>, Yun Yang<sup>b</sup>, Xiaomin Sun<sup>c</sup>, Jin Lin<sup>c</sup>, Ming Wu<sup>d</sup>, Jianfeng Wu<sup>a,\*</sup>, Jichun Wu<sup>a</sup>

4  
5 <sup>a</sup> Key Laboratory of Surficial Geochemistry, Ministry of Education; Department of  
6 Hydrosciences, School of Earth Sciences and Engineering, Nanjing University, Nanjing,  
7 210023, China

8 <sup>b</sup> School of Earth Sciences and Engineering, Hohai University, Nanjing, 210098, China

9 <sup>c</sup> Nanjing Hydraulic Research Institute, National Key Laboratory of Water Resources and  
10 Hydraulic Engineering, Nanjing, 210029, China

11 <sup>d</sup> Institute of Groundwater and Earth Sciences, Jinan University, Guangzhou, 510632, China

12

13

14

15

16 \*Corresponding author: Jianfeng Wu ([jfwu@nju.edu.cn](mailto:jfwu@nju.edu.cn); [jfwu.nju@gmail.com](mailto:jfwu.nju@gmail.com))

17

18

19 **ABSTRACT**

20 In the arid inland basins of China, the long-term unregulated agriculture irrigation from  
21 surface water diversion and groundwater abstraction has caused unsustainability of water  
22 resources and degradation of ecosystems. This requires integrated management of surface water  
23 (SW) and groundwater (GW) at basin scale to achieve scientific decision supports for sustainable  
24 water resources allocation in China. This study developed a novel multi-objective simulation-  
25 optimization (S-O) modeling framework. The optimization framework integrated a new epsilon  
26 multi-objective memetic algorithm ( $\epsilon$ -MOMA) with MODFLOW-NWT model to implement the  
27 real-world decision-making for water resources management while pondering the complicated  
28 groundwater-lake-river interaction in the arid inland basin. Then the optimization technique was  
29 validated through the SW-GW management in Yanqi Basin (YB), a typical arid region with  
30 intensive agricultural irrigation in northwest China. The management model, involving  
31 maximizations of total water supply rate, groundwater storage and surface runoff inflow to the  
32 terminal lake, and minimization of water delivery cost, was proposed to explore the tradeoffs  
33 between socioeconomic and environmental factors. It is shown that the tradeoff surface can be  
34 achieved in the 4-dimensional objective space by optimizing spatial groundwater abstraction in  
35 the irrigation districts and surface water diversion in the river. The Pareto-optimal solutions avoid  
36 the prevalence of decision bias caused by the low-dimensional optimization formulation.  
37 Decision-makers are then able to identify their desired water management schemes with  
38 preferred objectives and achieve maximal socioeconomic and ecological benefits simultaneously.  
39 Moreover, three representative runoff scenarios in relation to climate change were specified to  
40 quantify the effect of decreasing river runoff on the water management in YB. Results show that  
41 runoff depletion would be of great negative impact on the management objectives. Therefore,  
42 the integrated SW and GW management is of critical importance for the fragile ecosystem in YB  
43 under changing climatic conditions.

44 **Keywords:** Multi-objective optimization; Water resources management; Conjunctive use; Yanqi  
45 Basin; Bosten Lake

## 46 **1. Introduction**

47 In arid and semi-arid inland basins, the intensive irrigation for agricultural development  
48 caused the deterioration of natural ecosystem sustained with scarce water resources (Wichelns  
49 and Oster, 2006; Wu et al., 2016). In such cases, water managers are faced with choosing the  
50 optimal water supply scheme for the local economic development and eco-environmental  
51 conservation. In general, the pattern of water allocation in such regions incorporates groundwater  
52 (GW) abstraction from aquifer systems and surface water (SW) diversion from surface rivers  
53 (Liu et al., 2010; Wu et al., 2014). Hence, it is essential for the conjunctive management of GW  
54 and SW to deal with the contradiction between demand and supply of water resources in the arid  
55 regions with water shortage (Khare et al., 2006; Safavi and Esmikhani, 2013; Singh, 2014;  
56 Hassanzadeh, et al., 2014; Wu et al., 2016).

57 In the water resources planning and management, the simulation-optimization (S-O)  
58 methods can provide optimal schemes to guide and inform stakeholders (Maier et al., 2014). In  
59 the S-O framework, the simulation model explains the physical behaviors of water resources  
60 system and the management model explains the evaluation criteria of the water supply options  
61 (Singh, 2014). The management model includes objective functions as the performance metric  
62 of candidate schemes and constraint conditions defining the feasible decision space. However,  
63 the real-world water management problems are often complex, and associated with nonlinear  
64 and multimodal objectives and constraints. This complexity probably leads to the unavailability  
65 of the classical optimization algorithms such as mathematical programming and dynamic  
66 programming (Woodruff et al., 2013). For this reason, evolutionary algorithms have been  
67 extensively proved to be effective and reliable in solving the complex SW and GW management  
68 problems (McPhee and Yeh, 2004; Yang, et al., 2009; Safavi and Esmikhani, 2013; Singh and

69 Panda, 2013; Rothman and Mays, 2013; Wu et al., 2014; Parsapour-Moghaddam et al., 2015;  
70 Wu et al., 2016). Yang et al. (2009) considered conflicting bi-objectives with the conjunctive use  
71 of GW and SW to achieve optimal pumping and recharge schemes. Rothman and Mays (2013)  
72 developed an optimization model including cost control, aquifer protection and growth  
73 objectives using multi-objective genetic algorithm. Wu et al. (2016) performed the temporal  
74 optimization of monthly volume of surface water diverted from Heihe River by linking a  
75 physical-based integrated modeling with a simple single-objective management model. However,  
76 these studies rarely consider multi-objective optimization in the basin-scale water management  
77 with conjunctive use of SW and GW. The management model including the typical single  
78 objective or bi-objective formulation probably results in the decision bias (*i.e.*, cognitive myopia  
79 or short-sightedness) due to the sub-optimal solution only considering the fewer preference  
80 criteria (Kasprzyk et al., 2012, 2015; Woodruff et al., 2013; Matteo et al., 2019). Therefore, the  
81 water resources management with the strong and complex interactions between SW and GW  
82 calls for decision-maker to consider many-objective optimization that refers to the system design  
83 with four or more objectives (Fleming et al., 2005).

84 Multi-objective evolutionary algorithms (MOEAs) can obtain the tradeoff solutions that  
85 cater to multiple competing objectives and reflect comprehensive decision information for  
86 practitioners in real-world applications (Reed et al., 2013; Beh et al., 2017; Eker and Kwakkel,  
87 2018; Maier et al., 2019). However, many-objective optimization often suffers from the  
88 domination resistance phenomenon (Purshouse and Fleming, 2007; Hadka and Reed, 2013),  
89 which shows that the diminishing Pareto-sorting capacity triggers many non-dominated solutions  
90 in the population and then results in stagnation of evolutionary search. In order to alleviate the  
91 difficulty, Borg MOEA (Hadka and Reed, 2013) employed auto-adaptive recombination  
92 operators to enhance the evolutionary search ability,  $\epsilon$ -box technique to ensure the diversity and  
93 adaptive population sizing scheme to avoid search stagnation. The hybrid MOEA framework,

94 namely multi-objective memetic algorithm, composed of the biological process of natural  
95 selection and cultural evolution capable of local refinement, was applied to overcome some  
96 shortcomings of the traditional MOEA (*e.g.*, slow convergence, inefficient termination criterion)  
97 (Sindhya et al., 2011; 2013). These state-of-the-art MOEAs have been extensively validated and  
98 evaluated in addressing multi-objective optimization problems. However, due to the diversity  
99 and complexity of real-world decision-making problems, the algorithms may be inefficient in  
100 maintaining the diversity and convergence of Pareto front simultaneously. For example, Zheng  
101 et al. (2016) implemented the comparison of NSGAI, SAMODE and Borg in designing water  
102 distribution systems. The result indicated that Borg can converge quickly to the Pareto-optimal  
103 front whereas decrease the diversity of solutions. Hence, further efforts should be focused on  
104 advancing the MOEAs. This study aims at developing a new MOEA, named epsilon multi-  
105 objective memetic algorithm ( $\epsilon$ -MOMA), which integrates the  $\epsilon$ -dominance archive process, the  
106 auto-adaptive recombination operator and a local search operator into the basic framework of  
107 NSGAI (Deb et al., 2002b). Then, the proposed multi-objective optimization framework is  
108 applied to solve the integrated management of SW and GW in Yanqi Bain (YB).

109 YB is a typical oasis in an arid inland basin located to the southern Tianshan Mountains in  
110 Xinjiang Province, northwest China. The surface water resources in YB is composed of Kaidu  
111 River and Bosten Lake, the largest freshwater inland lake in China (Wang et al., 2014; Zhou et  
112 al., 2015). Kaidu River, as the largest river in the basin, supplies the vast majority of surface  
113 water for agricultural irrigation and recharge for Bosten Lake (Gao and Yao, 2005; Liu et al.,  
114 2013; Yao et al., 2018). Therefore, surface water diversion in the river dominates the water  
115 balance in Bosten Lake, which is the main water source for the lower reaches of Tarim River  
116 where the serious water crisis has taken place. With the intensive agricultural development in the  
117 past decades, surface water diverted from Kaidu River can no longer meet crop water  
118 requirements. Hence, groundwater became the alternative water source for crop production

119 whereas the excessive groundwater abstraction has caused the deterioration of local ecosystem  
120 associated with the decline of groundwater level and altered the hydraulic interaction between  
121 GW and SW (Hu et al., 2007; Zhang et al., 2014; Tian et al., 2015, Yao et al., 2015). Current  
122 water resources regulations in YB have shown the low performance in maintaining regional  
123 water balance, *e.g.*, decline of lake level in Bosten Lake. Therefore, the spatial pattern of water  
124 utilization (*i.e.*, decision variables) should be regulated to satisfy the preferred management  
125 objectives. The pattern is composed of groundwater abstraction in irrigation districts and surface  
126 water diversion through the aqueduct system connected with the river. The management  
127 objectives comprise minimizing the capital and operation costs of water delivery, maximizing  
128 water use demands for agricultural development (*i.e.*, total volume of surface water and  
129 groundwater use) and environmental flow for hydro-ecosystem conservation (*i.e.*, the regional  
130 groundwater storage and surface runoff inflow to the terminal lake). This study implements the  
131 integrated management of SW and GW by investigating the performance of tradeoffs including  
132 environmental, economic, social factors in designing optimal water allocation schemes with the  
133 new optimization framework. To our knowledge, there are very few researches about the many-  
134 objective optimization for the conjunctive management of SW-GW involving complex  
135 groundwater-river-lake interactions in arid inland basins within S-O framework.

136 In the changing world, the optimized schemes probably exhibit low performance even  
137 unfeasible under the future conditions (Maier et al., 2016). In YB, Kaidu River mainly gains  
138 water from seasonal precipitation that runs off the mountainous landscape and snow and glacier  
139 that melts in the upper Tianshan Mountains region known as a main water tower in the Central  
140 Asia. Therefore, the runoff variation in Kaidu River, which is highly sensitive to the changes of  
141 precipitation and glacier mass loss dominated by the climate change, greatly affects the water  
142 resources and water cycle in the basin. Three representative runoff scenarios in relation to climate  
143 change are specified to explore the effects of runoff reduction in Kaidu River on the integrated

144 SW and GW management practices.

145 This study firstly constructed the multi-objective SW-GW management model to consider  
146 water demands and environmental benefits including regional groundwater storage and surface  
147 runoff inflow to the terminal lake. Then the spatial conjunctive optimization of surface water  
148 diversion and groundwater abstraction was implemented based on the proposed optimization  
149 framework. The optimization results demonstrate that decision-makers can achieve the Pareto-  
150 optimal schemes constrained by satisfying the water demands and sustaining the fragile  
151 ecosystem in the arid inland basin with strong and complex SW-GW interactions. The  
152 implication from the multi-objective optimization under the runoff reduction scenarios shows  
153 that the conservative water management options may be desired in the face of deep uncertainty  
154 associated with climate changes. The study results can also provide valuable insights for water  
155 allocation in other arid inland basins.

## 156 **2. Methodology**

157 As shown in Fig. 1, this study aims to develop a multi-objective decision-making  
158 framework to optimize the irrigation schemes of surface water diversion and groundwater  
159 abstraction for the integrated SW and GW management. The optimal schemes can assist water  
160 managers to achieve water demands and ensure water balance of ecosystem in the arid inland  
161 basin. The optimization framework includes three main modules and their details are stated in  
162 the following sections.



174 development requires enough irrigation water to ensure local economic development while the  
175 sustainability of ecosystem also needs to follow specific requirements for maintaining  
176 environmental flows. For example, the excessive surface water diversion can significantly  
177 reduce the runoff inflow to the terminal lake, which causes obvious decline of lake level and  
178 results in the degradation of local ecosystem associated with the lake. Meanwhile, immoderate  
179 exploitation of groundwater stored in the aquifer to offset the surface water shortage triggers a  
180 series of environment problems (*e.g.*, dramatic decrease of groundwater storage). Therefore, the  
181 conflict between agricultural development and environmental conservation constrained by water  
182 scarcity stimulates the local water resources authority to implement scientific water management  
183 practices. The water managers should consider the total water supply rate and the cost of water  
184 delivery from multiple sources as socioeconomic metrics, and describe the runoff inflow to the  
185 lake and groundwater storage as environmental metrics. Then, water managers can assess water  
186 use practices by weighing these preference criteria. The performances of all schemes are  
187 evaluated based on the well-calibrated numerical model. The detailed formulation of  
188 management model can be seen in Section 3.3. Finally, the optimization model formulates water  
189 use practices as decision variables, socioeconomic and environmental metrics as management  
190 objectives, practical limitation of water exploitation and water demands for ecosystem as  
191 constrained conditions for the basin-scale SW and GW management.

## 192 *2.2 Optimization approach*

### 193 2.2.1 Main algorithmic structure

194 Module II in the optimization framework (Fig. 1) illustrates the algorithmic process of  $\varepsilon$ -  
195 MOMA. The main steps can be recapitulated as follows:

196 **Step 1:** Generation of initial population:  $N_{pop}$  individuals are firstly sampled over the decision  
197 space using Latin Hypercube Sampling (LHS) that is an effective sample scheme to ensure the

198 uniform distribution of initial population.

199 **Step 2:** Evaluation process of objectives and constraints: The simulation model is run with the  
200 calibrated parameters. Then objectives and constraints are calculated from the model output  
201 variables (*i.e.*, state variables).

202 **Step 3:** Evolutionary operators for the creation of offspring population: The auto-adaptive multi-  
203 operator recombination proposed by Hadka and Reed (2013) is a promising technique to select  
204 the optimal operator for real-world optimization problems. The crossover probability of each  
205 operator is updated periodically based on the proportion of the solutions generated by each  
206 operator in the  $\varepsilon$ -dominance archive. The recombination strategy is essential for the intricate  
207 multi-objective optimization in the real-world problems due to the inability to know a priori the  
208 optimal recombination operator. This study integrated the six real-valued recombination  
209 operators (*i.e.*, simulated binary crossover (SBX) (Deb and Agrawal, 1994), differential  
210 evolution (DE) (Storn and Price, 1997), simplex crossover (SPX) (Tsutsui et al., 1999), parent-  
211 centric crossover (PCX) (Deb et al., 2002a), Laplace crossover (LX) (Deep and Thakur, 2007),  
212 uniform mutation (UM)) into the  $\varepsilon$ -MOMA to enhance the potential of evolutionary search in  
213 higher order objective spaces. Additionally, the polynomial mutation is applied to the  
214 recombination population.

215 **Step 4:**  $\varepsilon$ -domination archive process: The  $\varepsilon$ -box technique proposed by Laumanns et al. (2002)  
216 attempts to ensure convergence and diversity of the approximate Pareto-optimal solutions.  
217 Moreover, decision-makers can define the minimum resolution of objective vector with epsilon  
218 vector to satisfy their acceptable precision target and restrict the archive size. This study  
219 implemented the  $\varepsilon$ -dominance archive process after the fast non-dominated sorting of offspring  
220 individuals and alleviated the difficulties derived from the domination resistance in the many-  
221 objective optimization.

222 **Step 5:** Bidirectional local mutation: The archived solutions are operated based on Gaussian

223 perturbation in the neighborhood of decision variables. Given an archived individual  
 224  $\mathbf{v}=(v_1,v_2,v_3,\dots,v_n)$ , the mutated individuals can be stated as:

$$225 \quad \mathbf{v}^+ = (v_1, v_2, \dots, v_i + p \times (m_i - w_i), \dots, v_n) \quad (1)$$

$$226 \quad \mathbf{v}^- = (v_1, v_2, \dots, v_i - p \times (m_i - w_i), \dots, v_n) \quad (2)$$

227 where  $\mathbf{v}=(v_1,v_2,\dots,v_n)$  is an  $n$ -dimensional decision variable vector;  $\mathbf{m}=(m_1,m_2,\dots,m_n)$  and  
 228  $\mathbf{w}=(w_1,w_2,\dots,w_n)$  are two individuals randomly selected from the archive;  $c$  follows standard  
 229 Gaussian distribution. The process is effective with the probability of  $1/n$  (Chen et al., 2015).  
 230 The algorithm revives the local search operator in every several generations and then updates the  
 231 archive again.

232 **Step 6:** Return to Step 2 if the termination criterion is not satisfied. This study specified the  
 233 number of function evaluations as termination condition.

234 In the many-objective optimization,  $\varepsilon$ -MOMA utilizes the  $\varepsilon$ -dominance concept to archive  
 235 elite individuals for the maintenance of diversity and the auto-adaptive recombination operator  
 236 with local search for the enhancement of convergence on the basis of the framework of NSGAII.  
 237 Hence, the algorithm possesses the ability of highly effective global search with auto-adaptive  
 238 recombination operator and  $\varepsilon$ -dominance archive to find higher quality and diverse solutions  
 239 with local search operator.

#### 240 2.2.2 Benchmark test

241 To investigate the performance of  $\varepsilon$ -MOMA in the many-objective optimization, we  
 242 implement benchmark test with the 3 to 6 objectives DTLZ1 and DTLZ3 problems (Deb et al.,  
 243 2002c). The test instances are deceptive and probably converge to the sub-optimal Pareto front,  
 244 which provides a severe challenge for the algorithm to get close to the global Pareto-optimal  
 245 front. The hypervolume metric (HV) is applied to evaluate the convergence and diversity of  
 246 approximate Pareto front (Zitzler et al., 2003). The global Pareto-optimal front for DTLZ

247 problems is known and can be considered as the reference set. The HV metric indicates the  
248 dominated region of the non-dominated solutions relative to the reference point that is the extent  
249 of the reference set. The HV of the reference set ( $HV_{rs}$ ) and the approximate set ( $HV_{as}$ ) can be  
250 calculated using a fast search algorithm proposed by Bader and Zitzler (2011) in the high-  
251 dimensional objective space. This study uses the normalized HV (*i.e.*,  $HV_n = HV_{as}/HV_{rs}$ ) to  
252 evaluate the performance of  $\varepsilon$ -MOMA for these test problems. The approximate Pareto front  
253 completely converges to the reference set when  $HV_n$  is equal to one. The test results show that  $\varepsilon$ -  
254 MOMA is capable of achieving a larger value of  $HV_n$  metric (over 95%), indicating that the  
255 approximate Pareto front is very close to the global optimal Pareto front (Table S1 in the  
256 Supplementary Materials). In higher-dimensional objective space, the performance of  $\varepsilon$ -MOMA  
257 can be maintained by augmenting the number of function evaluations. Therefore, the proposed  
258  $\varepsilon$ -MOMA is effective in addressing many-objective optimization from the benchmark test.

### 259 *2.3 Visual analytics of Pareto-front*

260 In the many-objective optimization, it is difficult for water managers to distinguish the  
261 performance of single solution and discover desired schemes without the interactive visual  
262 analytics. Module III used a visual analytics package, DiscoveryDV (Hadka et al., 2015; Kollat  
263 and Reed, 2007), to explore and analyze water management practices in the high-order objective  
264 spaces. The package employed multi-dimensional coordinate plot and parallel coordinate plot  
265 (Inselberg, 2009) to visualize Pareto solutions. Visualizing performance objectives can assist  
266 stakeholders to compare with the scheme before optimization and select key tradeoff schemes  
267 with a clearer perspective (Matteo et al., 2019; Maier et al., 2014). Moreover, decision-makers  
268 can eliminate redundant schemes with the preferred objectives or concerns and filter the optimal  
269 subsets those probably adopted by the experienced practitioners.

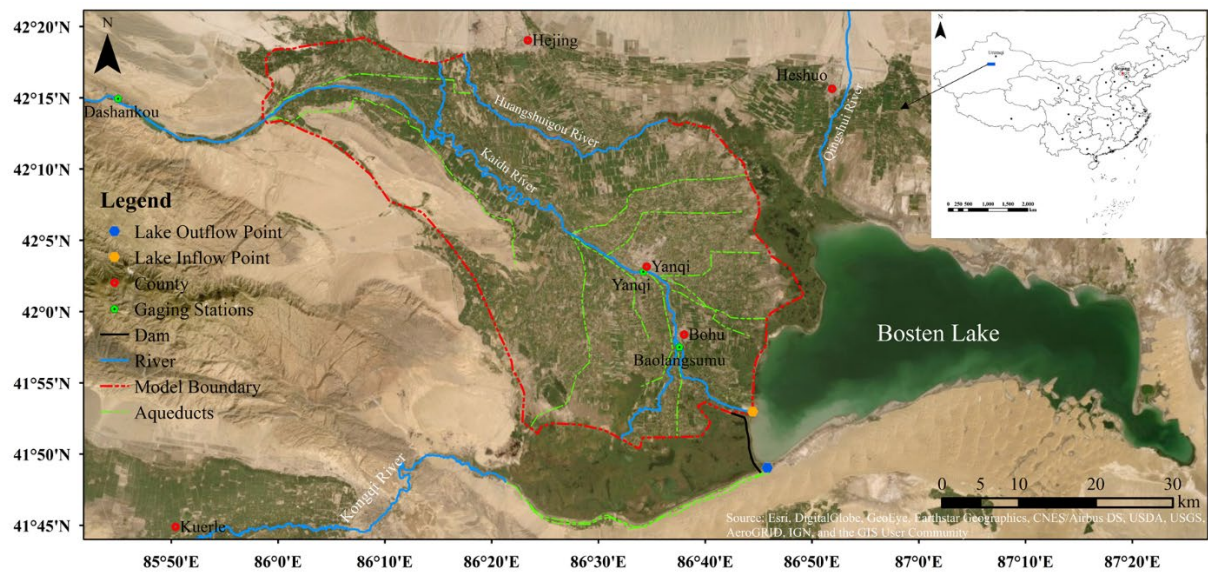
## 270 3 Case study

### 271 3.1 Study area

272 YB is a typical oasis in an arid inland desert basin in the southern Tianshan Mountains,  
273 Xinjiang Province, northwest China and includes Yanqi County, Hejing County, Bohu County  
274 and Heshuo County, with a total area of about 7600 km<sup>2</sup> (Fig. 2). In the model domain, the  
275 northwest is mountainous and the south is a low-lying desert, and the terrain slopes from  
276 northwest to lower southeast. YB is located in the temperate zone of continental desert climate  
277 with an annual mean temperature of 14.6 °C, an annual precipitation of 50.7-79.9 mm, and a  
278 potential evaporation of 2000.5-2449.7 mm (Mamat et al., 2014). The basin is mainly composed  
279 of Kaidu River, Huangshuigou River and Qingshui River. Kaidu River originates from the Hargat  
280 Valley and the Jacsta Valley in the middle part of the Tianshan Mountain with a maximum  
281 altitude of 5000 m and ends in Bosten Lake (Xu et al., 2016). Kaidu River is the largest river in  
282 YB which provides annual mean runoff of 3.41 billion m<sup>3</sup> (Wang et al., 2013) and plays an utmost  
283 role in protecting the lake and its surrounding ecology and environment. The Dashankou station  
284 is the dividing point that divides the mainstream of the river into middle and lower reaches. In  
285 YB, the runoff in Kaidu River is mainly diverted for agricultural irrigation and finally flows into  
286 Bosten Lake, which contributes to about 95% of the water recharge for the lake (Yao et al., 2018).  
287 Bosten Lake is a largest freshwater inland lake in China covering the area of about 1005 km<sup>2</sup>  
288 with a length of 55 km and a width of 25 km. The lake water volume is approximately 8.80  
289 billion m<sup>3</sup>, with an average depth of 7 m and a maximum depth of 17 m (Xiao et al., 2010). The  
290 evaporation and an artificial discharge by a pumping station built in 1983 control the outflow of  
291 the lake. As shown in Fig. 2, the pumping channel starting from the outflow point is used to  
292 divert the lake water to recharge Kongqi River and supply water to the lower Tarim River. The  
293 dam is built to sustain higher lake level for the water diversion. Therefore, Bosten Lake is a main

294 water source to the lower reaches of Tarim River, which has suffered from severe degradation of  
295 ecological environment resulted from unregulated water exploitation in the past decades. In order  
296 to regenerate “Green Corridor” in the lower reaches of Tarim River, Chinese government has  
297 implemented the Ecological Water Conveyance Project since 2000 to increase the recharge of  
298 groundwater system that is crucial for the growth of natural vegetation (Xu et al., 2007; Hao and  
299 Li, 2014). As illustrated in Fig. S1, the project firstly transfers water through Kongqi River from  
300 Bosten Lake to Daxihaizi Reservoir and then to the lower reaches of Tarim River, and finally to  
301 the terminal lake (Chen et al., 2010). However, YB is an intensive agricultural area where is  
302 mostly made up of farmland growing crops of tomato and pepper. The irrigation water demands  
303 accounted for 90% of the total water consumption in the basin due to the rapid increase of  
304 farmland area in the recent years (Yao, et al., 2018). Consequently, the scientific water  
305 management strategies should strike for balancing the demands of existing irrigation and eco-  
306 environmental water use to sustain enough water inflowing from Kaidu River to the lake and the  
307 regional aquifer.

308 This study selects the core part of YB comprising the majority of irrigation districts and  
309 Kaidu River. The river plays a vital role in regulating and maintaining regional water balance in  
310 the basin. The model domain (Fig. 2) is bounded by the mountains on the northwest,  
311 Huangshuigou River on the northeast, swamp areas and Bosten Lake on the south. As shown in  
312 Fig. 2, an aqueduct system conveys and redistributes the surface runoff from the mainstream of  
313 Kaidu River and the wells are used to pump groundwater in the aquifer system.

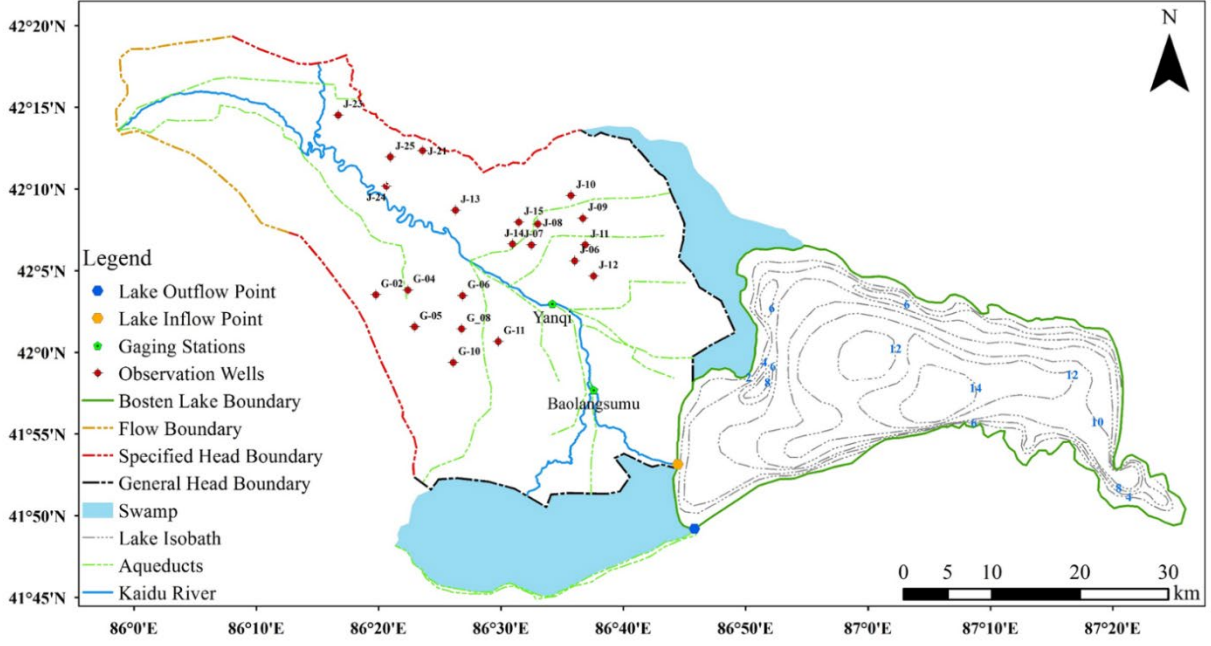


314  
 315 **Fig. 2.** The location of Yanqi Basin and the model domain of interest for this study. Source: DigitalGlobal,  
 316 Inc. (imagery).

317 *3.2 Numerical model*

318 The numerical model in this study is modified from the previous work of Wu et al. (2018)  
 319 using MODFLOW-NWT. The program applies the Newton-Raphson formulation and  
 320 unstructured, asymmetric matrix solvers to solving drying and rewetting nonlinearities of the  
 321 complex unconfined groundwater flow problem (Niswonger, 2011) while supports most modular  
 322 packages in MODFLOW-2005 (Harbaugh, 2005). Then we perform a multi-objective  
 323 optimization with the corrected model. The specified boundary conditions in the model are  
 324 illustrated in Fig. 3. The northwest border was defined as the flow boundary to simulate recharge  
 325 of groundwater runoff in the interface between mountains and plain. Huangshuigou River and  
 326 southwest border were considered as the specified head boundary based on observed  
 327 groundwater level. The swamps and Bosten Lake were modelled using the General Head  
 328 Boundary (GHB) package and Lake package (LAK3) (Michael and Leonard, 2000), respectively.  
 329 LAK3 package models the lake and aquifer interactions by calculating the exchange rate, which  
 330 is determined by the difference between lake level and groundwater, the hydraulic conductivity  
 331 of adjacent aquifer and the material of lakebed. The lake level responses to the hydraulic stresses

332 including lake atmospheric recharge and evaporation, overland runoff, and any direct withdrawal  
333 or recharge of the lake volume. The bathymetric contours of Bosten Lake were used to confirm  
334 the lake bottom topography. Kaidu River and aqueducts were simulated using the Streamflow-  
335 Routing package (SFR2) (Richard and David, 2010). SFR2 package, as a modular package in  
336 MODLFOW-NWT, can be used to model the interactions between streams and underlying  
337 aquifer while consider unsaturated flow beneath streams for the disconnected river. The  
338 streamflow is routed based on the continuity equation assuming steady and uniform flow. The  
339 Manning's Equation and Darcy's Law are used to represent the relation between river stage and  
340 discharge and calculate the infiltration/exfiltration rate between streams and aquifers,  
341 respectively. The simulation period in the transient model was defined from November in 2003  
342 to October in 2013. Totally 20 stress periods were discretized, two periods for each year  
343 including non-irrigation period (from November to next March) and irrigation period (from April  
344 to October of each year), over the entire simulation period. The key parameters for both SW and  
345 GW were adjusted to reproduce the fluctuation of groundwater levels at the observation wells  
346 and streamflow in the gaging stations (*i.e.*, Yanqi and Baolangsumu stations). The observed lake  
347 levels in the simulation period were employed to calibrate the numerical model. The more data  
348 details can be found in Table S2.



349  
 350 **Fig. 3.** The boundary conditions of model domain, monitoring locations of groundwater level and surface  
 351 runoff, aqueduct system and bathymetric contours in meters for Bosten Lake.

352 The model calibration was manually implemented by the trial-and-error method. The Nash-  
 353 Sutcliffe Efficiency (NSE) was applied to evaluate the simulated precision of runoff and lake  
 354 level. The predicted precision of groundwater head was assessed based on root mean square error  
 355 (RMSE) and correlation coefficient ( $R$ ). The performance criteria can be stated as:

356 
$$NSE = 1 - \frac{\sum_{t=1}^T (y_{m,t} - y_{o,t})^2}{\sum_{t=1}^T (y_{o,t} - \bar{y}_o)^2} \quad (3)$$

357 
$$RMSE = \sqrt{\sum_{i=1}^N (y_{m,i} - y_{o,i})^2 / N} \quad (4)$$

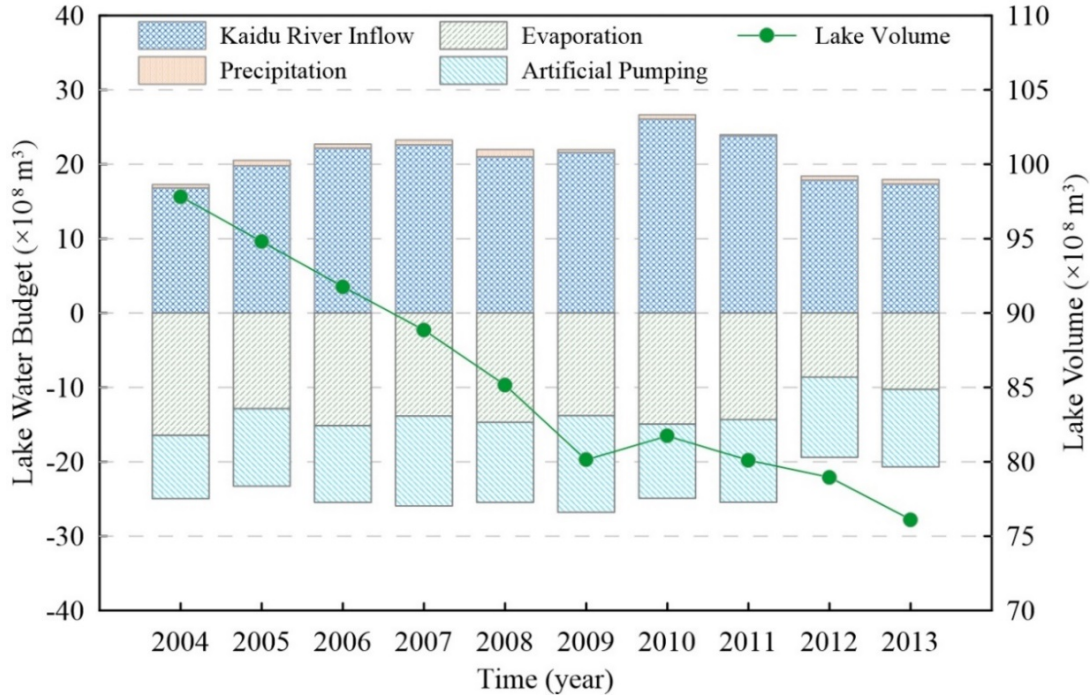
358 
$$R = \frac{\sum_{i=1}^N (y_{m,i} - \bar{y}_m)(y_{o,i} - \bar{y}_o)}{\sqrt{\sum_{i=1}^N (y_{m,i} - \bar{y}_m)^2 \times \sum_{i=1}^N (y_{o,i} - \bar{y}_o)^2}} \quad (5)$$

359 where  $y_{m,t}$  and  $y_{o,t}$  are the simulated and observed runoff or lake level for  $t$ th stress period,  
 360 respectively;  $T$  is the number of stress periods;  $y_{m,i}$  and  $y_{o,i}$  are the simulated and observed

361 groundwater head at the  $i$ th observation well, respectively;  $N$  is the number of observation wells;  
362  $\bar{y}_m$  and  $\bar{y}_o$  are the average value of simulated and observed data. Fig. S2a and S2b compare  
363 the simulated and observed runoff at Yanqi and Baolangsumu Stations for the stress periods  
364 between 2004 and 2012 (lack of observed runoff in 2013) and suggest that the long-term  
365 fluctuation of runoff in Kaidu River can be well reproduced with NSE of 0.89 and 0.90,  
366 respectively. Fig. S2d shows the simulated groundwater heads have a good-fit with observed  
367 heads at all observation wells with RMSE of 1.8 m and R of 0.98. Fig. S2e compares the observed  
368 and calibrated groundwater level over time in the three observation wells and the groundwater  
369 variation trend in the irrigation and non-irrigation period can be achieved.

370 The interaction between Bosten Lake and the aquifer is dominated by the hydraulic  
371 conductivity of the lakebed, of which value is very small owing to the existence of the thick low-  
372 permeability sediment in the region. The main inflow term of the lake is the surface runoff from  
373 Kaidu River which has been calibrated with the runoff data in the gauging stations. The recharge  
374 for the lake from precipitation is not significant in the arid inland basin. The outflow terms are  
375 mainly composed of the evaporation and artificial pumping to divert water from the lake to  
376 Kongqi River. The local water resources authority in YB provided the data of artificial pumping  
377 in the simulation period. However, the average evaporation in Bosten Lake calculated using  
378 potential evaporation data or Penman's equation is not accurate because the temperature and  
379 relative humidity exhibit the significant difference over the approximately 945.0 km<sup>2</sup> evaporation  
380 surface. Therefore, the observed lake stages were applied to calibrate evaporation rate in the lake.  
381 Fig. S2c illustrates the calibration results of lake level (NSE=0.97) and indicates that the decline  
382 trend of lake level can be adequately captured. Then, the water balance of Bosten Lake can be  
383 achieved as shown in Fig. 4. In the simulation period from 2004 to 2013, surface runoff inflow  
384 in Kaidu River represents 97.4% of the total annual inflow to Bosten Lake. The total annual  
385 outflow of the lake consists of 54.9% of lake evaporation and 44.2% of artificial pumping.

386 Therefore, the surface runoff in Kaidu River is a crucial factor to maintain the water balance of  
 387 Bosten Lake. The surface runoff inflow can be considered as a significant performance metric to  
 388 evaluate the water use practices in the basin. Finally, the well-calibrated model can be employed  
 389 to integrated SW and GW management.

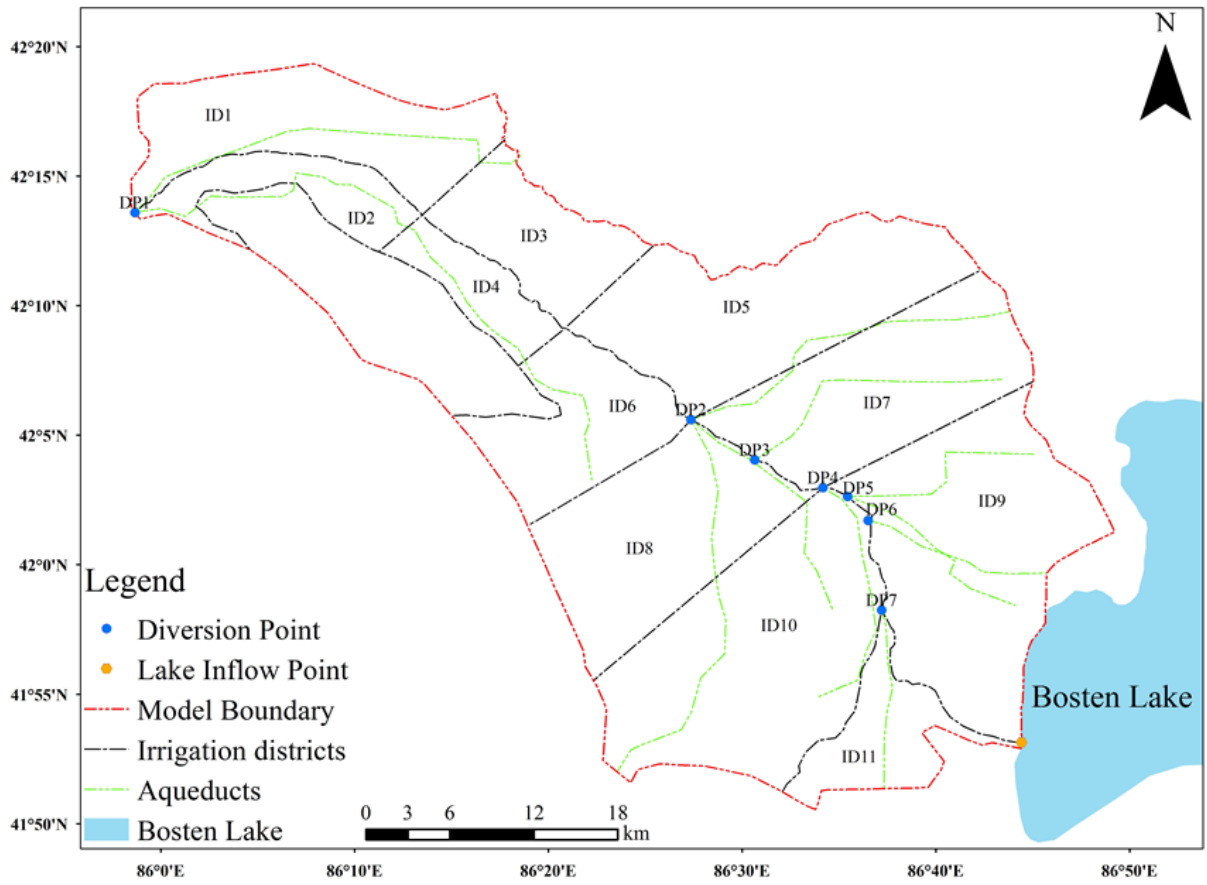


390  
 391 **Fig. 4.** The water balance terms of Bosten Lake and resulting lake volume in the simulation period.

392 *3.3 Management model*

393 The integrated SW and GW management focuses on not only the water resources  
 394 exploitation subject to social and economic benefits but also the effect of water exploitation on  
 395 environment benefits. The study formulated an integrated SW and GW optimization problem  
 396 including four management objectives: (1) to maximize total water supply rate ( $f_{TWS}$ ); (2) to  
 397 minimize total cost of water delivery from water intake points to water use destinations ( $f_{TCOST}$ );  
 398 (3) to maximize the groundwater storage change of saturated zone between the beginning and  
 399 end of management period ( $f_{GSC}$ ) which is negative when the storage decreases and vice versa;  
 400 and (4) to maximize surface runoff inflow from Kaidu River to Bosten Lake ( $f_{SRI}$ ).  $f_{TWS}$  and  $f_{TCOST}$   
 401 are defined as the metrics to satisfy the local irrigation water demands while maintain the lower

402 costs of water use.  $f_{GSC}$  is formulated as the metric indicating the extent of groundwater  
 403 abstraction and a greater value shows a preferred situation.  $f_{SRI}$  is defined to evaluate the  
 404 influence of surface runoff from Kaidu River on the water balance in Bosten Lake, which  
 405 contributes about 97.4% of the total inflow (Fig. 4). As shown in Fig. 5, the decision variables  
 406 are the total volume of surface water diverted in the mainstream of Kaidu River in the diversion  
 407 point (DP1-DP7) and groundwater abstraction in the irrigation districts (ID1-ID11).



408  
 409 **Fig. 5.** The locations of surface water diversion points and subdomains of irrigation districts for groundwater  
 410 abstraction.

411 The formulations of management model are given as follows:

412 
$$\text{Max } f_{TWS} = \sum_{i=1}^{N_p} Q_{g,i} + \sum_{i=1}^{N_d} Q_{s,i} \quad (6)$$

413 
$$\text{Min } f_{TCOST} = \sum_{k=1}^{N_t} \sum_{i=1}^{N_w} q_{g,i,k} C_g (H_i - h_{i,k}) T_k + \sum_{k=1}^{N_t} \sum_{i=1}^{N_d} q_{s,i,k} C_s T_k \quad (7)$$

414 
$$\text{Max } f_{GSC} = \sum_{j=1}^{N_g} (h_{end,j} - h_{ini,j}) Sy_j A_j \quad (8)$$

415 
$$\text{Max } f_{SRI} = f_{gaging}(\mathbf{X}) \quad (9)$$

416 
$$\mathbf{X} = (Q_{g,1}, Q_{g,2}, \dots, Q_{g,N_p}; Q_{s,1}, Q_{s,2}, \dots, Q_{s,N_d}) \quad (10)$$

417 where  $Q_{g,i}$  is total groundwater abstraction rate at  $i$ th irrigation district ( $\text{m}^3/\text{yr}$ );  $Q_{s,i}$  is total volume  
 418 of surface water diverted from  $i$ th diversion point ( $\text{m}^3/\text{yr}$ );  $N_p$  is the number of irrigation districts;  
 419  $N_d$  is the number of diversion point based on the locations of aqueducts;  $N_t$  is the number of  
 420 stress period including irrigation and non-irrigation period;  $N_w$  is total number of pumping wells;  
 421  $q_{g,i,k}$  is the pumping rate at the  $i$ th well in  $k$ th stress period ( $\text{m}^3/\text{d}$ );  $C_g$  is the cost per unit pumping  
 422 rate per length of hydraulic lift in case of wells ( $0.015 \text{ CNY}/\text{m}^3/\text{m}$ ), and CNY stands for Chinese  
 423 Yuan;  $H_i$  is the surface elevation at the  $i$ th pumping well (m);  $h_{i,k}$  is the groundwater level at the  
 424  $i$ th well in  $k$ th stress period (m);  $T_k$  is the length of the  $k$ th stress period (d);  $q_{s,i,k}$  is the surface  
 425 water diversion rate at the  $i$ th diversion point in  $k$ th stress period ( $\text{m}^3/\text{d}$ );  $C_s$  is the cost per unit  
 426 diversion volume ( $0.055 \text{ CNY}/\text{m}^3$ );  $N_g$  is the total number of active cell in the model domain;  
 427  $h_{end,j}$ ,  $h_{ini,j}$  is the groundwater level at the end and beginning of management period (m);  $Sy_j$  is  
 428 the specific yield at  $j$ th active cell;  $A_j$  is the area of  $j$ th grid cell ( $\text{m}^2$ );  $f_{gaging}$  outputs the surface  
 429 runoff in Kaidu River at the inflow point of Bosten Lake ( $\text{m}^3/\text{d}$ );  $\mathbf{X}$  is a water use scheme.

430 The management model consists of a set of constraints given by:

431 
$$Q_{g,min} \leq Q_{g,i} \leq Q_{g,max} \quad Q_{s,min} \leq Q_{s,i} \leq Q_{s,max} \quad (11)$$

432 
$$d_{max} \leq d_c \quad h_{lake} \geq h_c \quad (12)$$

433 
$$\sum_{i=1}^{N_p} Q_{g,i} \geq TP_{min} \quad \sum_{i=1}^{N_d} Q_{s,i} \geq TD_{min} \quad (13)$$

434 
$$Q_{out,i} > 0.0 \quad (14)$$

435 where  $Q_{g,min}$  and  $Q_{g,max}$  are the capacity of total groundwater abstraction at specified irrigation

436 district and  $Q_{g,min}$  is uniformly assumed to 1.0 million  $m^3/yr$  ( $Mm^3/yr$ ) and  $Q_{g,max}$  is 100.0  $Mm^3/yr$ ;  
437  $Q_{s,min}$  and  $Q_{s,max}$  are the constraints of surface water diversion at diversion point,  $Q_{s,min}$  is 10.0  
438  $Mm^3/yr$  at diversion points DP1 and DP2 and 5.0  $Mm^3/yr$  at DP3-DP7,  $Q_{s,max}$  is 400.0  $Mm^3/yr$   
439 at DP1 and 200.0  $Mm^3/yr$  at DP2 and 100.0  $Mm^3/yr$  at DP3-DP7;  $d_{max}$  is the maximum  
440 drawdown and must less than the permission value  $d_c$  which is set to 5 m based on the existing  
441 management schemes;  $h_{lake}$  is lake level and must greater than minimum level  $h_c$  (1045 m in this  
442 study) to divert lake water to recharge Kongqi River;  $TP_{min}$  and  $TD_{min}$  is the prescribed minimum  
443 water demands of total groundwater abstraction and total surface water diversion to satisfy the  
444 agricultural development and are set to 300.0  $Mm^3/yr$  and 550.0  $Mm^3/yr$  based on the reports  
445 from the local water resources authority;  $Q_{out,i}$  represents outflow of the end reach of  $i$ th stream  
446 segment and must greater than zeros which means the potential diversion at each diversion point  
447 does not exceed the available streamflow in the current segment to avoid significant error of  
448 water budgets in the optimization (Wu et al., 2015). This study aims at optimizing spatial  
449 distribution of groundwater abstraction at different irrigation district and surface water diversion  
450 at each diversion point. The management period was set to one year with duplicated model inputs  
451 and parameters from November 2012 to October 2013 including the non-irrigation and irrigation  
452 periods. Then the conjunctive management of SW and GW is implemented based on the multi-  
453 objective optimization framework carried out in MATLAB software  
454 (<http://www.mathworks.com/products/matlab>).

## 455 **4 Results and discussion**

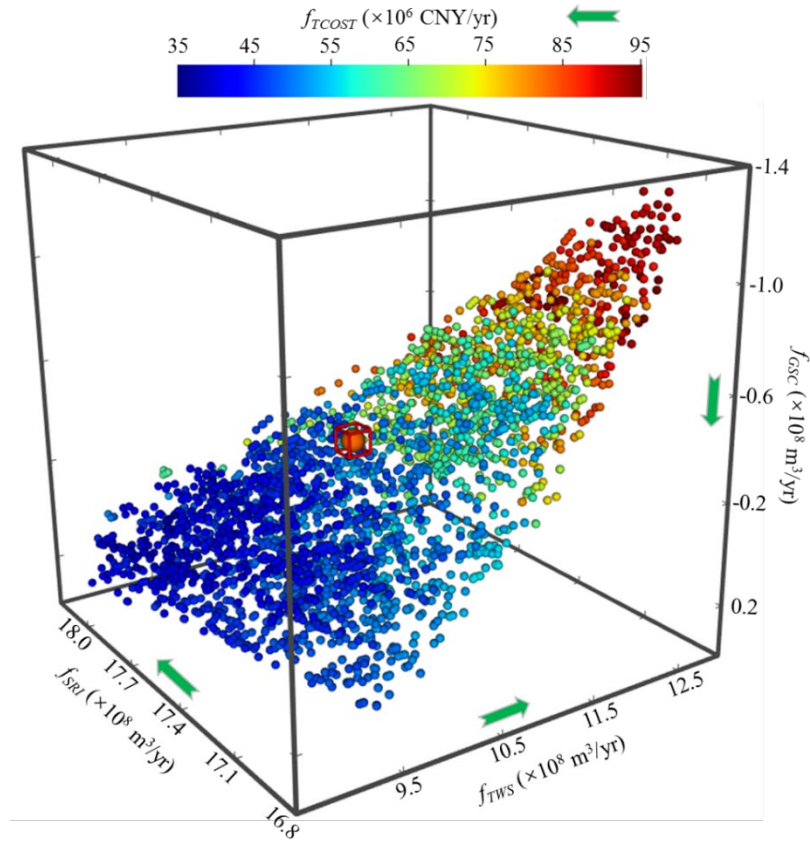
### 456 *4.1 Pareto-optimal solutions*

457 This study applied  $\epsilon$ -MOMA to solve the integrated SW and GW management model with  
458 four objectives ( $f_{TWS}$ ,  $f_{TCOST}$ ,  $f_{GSC}$  and  $f_{SRI}$ ) to search for optimal water use schemes. The algorithm  
459 parameters and objective epsilon values are summarized in Table 1. Fig. 6 shows a global view

460 of tradeoff surface in a 4-dimensional coordinate plot. The management model consists of  
461 maximizing the  $f_{TWS}$ ,  $f_{GSC}$  and  $f_{SRI}$  objectives and minimizing the  $f_{TCOST}$  objective. The  $f_{TWS}$ ,  $f_{SRI}$   
462 and  $f_{GSC}$  are plotted on the  $x$ ,  $y$  and  $z$  axes and  $f_{TCOST}$  is represented with color in Fig. 6. The green  
463 arrow indicates the direction of optimality in each objective. It can be observed that the trade-off  
464 relationship exists between  $f_{TWS}$  and other objectives ( $f_{TCOST}$ ,  $f_{GSC}$  and  $f_{SRI}$ ). Augmenting the total  
465 amount of water supply increases the cost of transporting water with the solutions marked in red  
466 color and reduces surface runoff inflow to the lake and groundwater storage at the end of  
467 management period. Therefore, the regional water resources exploitation conflicts with the  
468 socioeconomic and environmental benefits in YB. The scheme before optimization is marked in  
469 red square box in Fig. 6. We can see that the scheme is located above the tradeoff surface and  
470 exhibits larger cost value. Thus, the current management scheme is sub-optimal and can be  
471 regulated to obtain optimal performances.

472 **Table 1.** The control parameters of  $\epsilon$ -MOMA and epsilon value of objectives

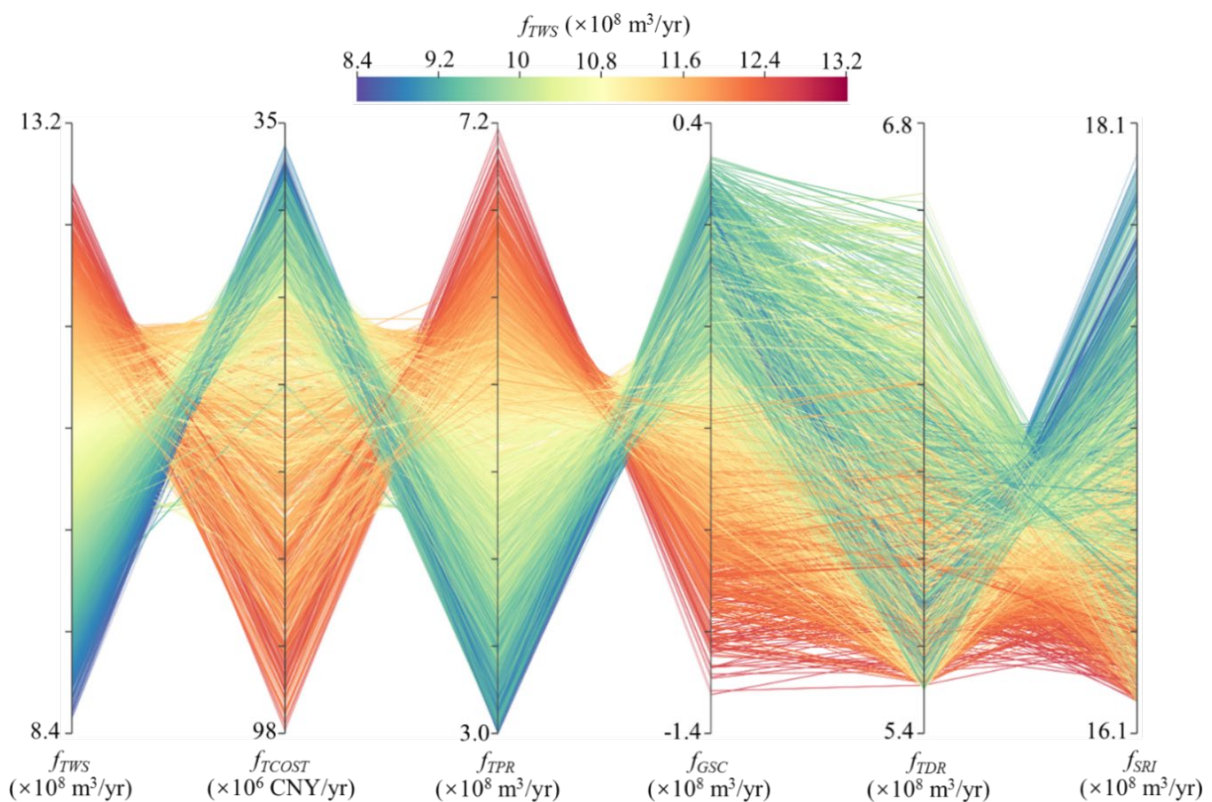
Parameter	Value
Population size ( $N_{pop}$ )	200
Maximum function evaluation ( $N_{eval}$ )	$6 \times 10^4$
Crossover probability ( $P_c$ )	0.90
Mutation probability ( $P_m$ )	0.05
$f_{TWS}$ epsilon ( $m^3/yr$ )	$1 \times 10^4$
$f_{TCOST}$ epsilon (CNY/yr)	$1 \times 10^2$
$f_{GSC}$ epsilon ( $m^3/yr$ )	$1 \times 10^4$
$f_{SRI}$ epsilon ( $m^3/yr$ )	$1 \times 10^4$



473  
 474 **Fig. 6.** The tradeoff surface to the integrated SW-GW management in Yanqi Basin. Each spheric symbol  
 475 represents a water use scheme corresponding to specific objective values of the total water supply rate ( $f_{TWS}$ ),  
 476 total cost of water delivery ( $f_{TCOST}$ ), surface runoff inflow to lake ( $f_{SRI}$ ) and groundwater storage change ( $f_{GSC}$ ).  
 477  $f_{TCOST}$  is symbolized in color to identify the objective value against others. The green arrow is the direction of  
 478 better performance for each objective. The scheme before optimization is marked in a red square box.

479 To explain the discrepancy of the Pareto-optimal solutions, the parallel coordinates (PC) is  
 480 used to explore the tradeoff surface. PC is composed of  $N$  equal-spaced parallel axes representing  
 481  $N$ -dimensional objective vector. Each polyline intersecting its axis in terms of objective value  
 482 represents the decision scheme in the Pareto-optimal solutions. Meanwhile, the total pumping  
 483 rate ( $f_{TPR}$ ) and total surface water diversion rate ( $f_{TDR}$ ) are added to elucidate the effect of  
 484 conjunctive use of SW and GW. In Fig. 7, the segments with higher  $f_{TWS}$  exist for higher  $f_{TCOST}$   
 485 and lower  $f_{GSC}$  and  $f_{SRI}$ , showing that increasing water demands requires more financial  
 486 investment and depletes more surface runoff inflow to the lake and groundwater storage. The  
 487 findings are consistent with the previous inferences in Fig. 6. Moreover, the many slope segments

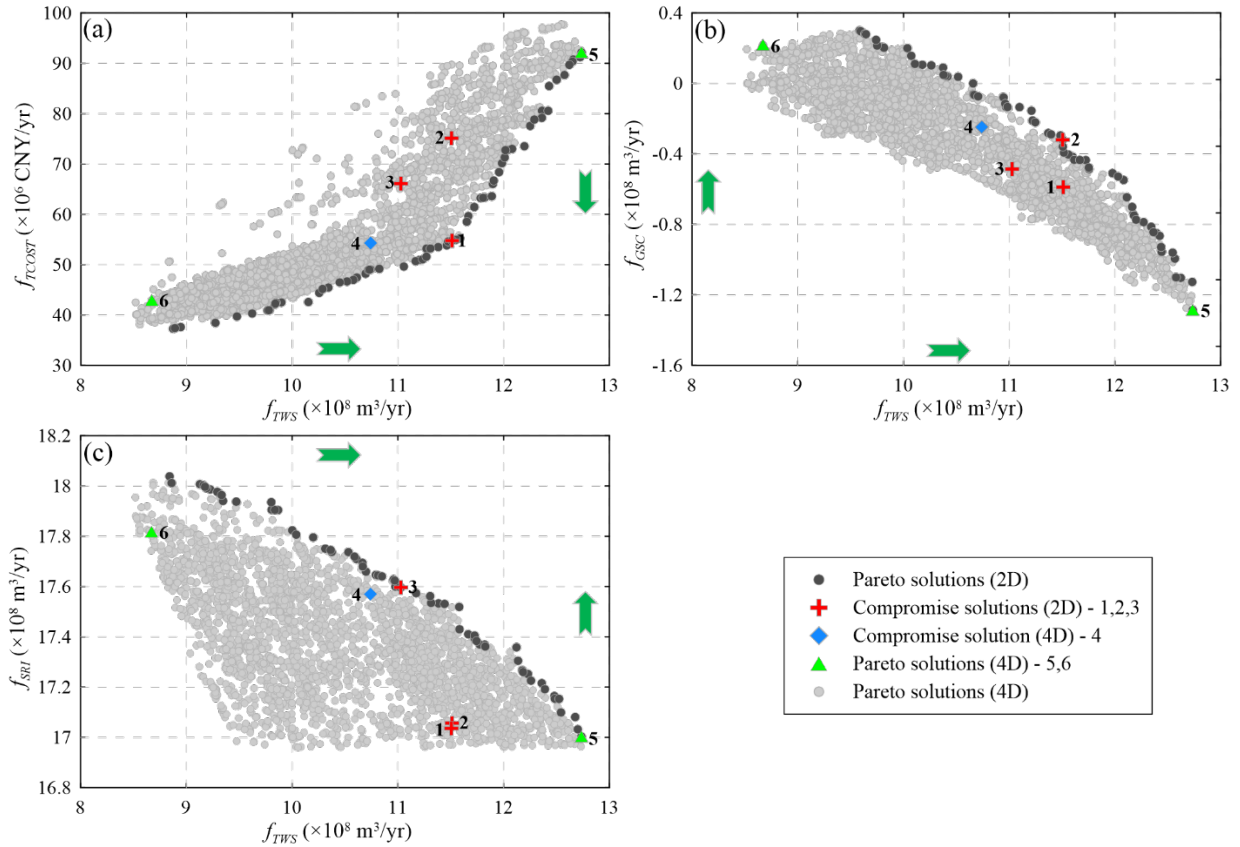
488 exist between  $f_{TPR}$  and  $f_{GSC}$ ,  $f_{TDR}$  and  $f_{SRI}$ , which indicates that enlarging groundwater abstraction  
 489 and surface water diversion are the dominated factors for the depletion of groundwater storage  
 490 and surface runoff recharge for the lake, respectively. It is noteworthy that the variation trend of  
 491  $f_{TPR}$  is very close to the change of  $f_{TWS}$  while the change in  $f_{TDR}$  exists obvious difference. The  
 492 increment of  $f_{TPR}$  can be reached to 416.0 Mm<sup>3</sup>/yr whereas the growth of  $f_{TDR}$  only is 114.0  
 493 Mm<sup>3</sup>/yr across all the Pareto solutions. Therefore, groundwater abstraction can be adjusted  
 494 largely to satisfy management objectives based decision-makers' preference whereas surface  
 495 water diversion should be restricted. The reasons behind this bias are that surface water diversion  
 496 is highly sensitive to the lake level and the intensive groundwater abstraction augments the river  
 497 leakage that indirectly causes the decrease of available runoff.



498  
 499 **Fig. 7.** The objective values ( $y$ -axis) are plotted over management objectives  $f_{TWS}$ ,  $f_{TCOST}$ ,  $f_{GSC}$ ,  $f_{SRI}$ , total  
 500 pumping rate  $f_{TPR}$  and total surface water diversion rate  $f_{TDR}$  ( $x$ -axis),  $f_{TWS}$  is represented in color. The preferred  
 501 direction for each index is upward.

## 502 4.2 Optimized management schedule

503 The superiority in many-objective optimization is the full exploration of optimal solutions  
504 to avoid the decision bias derived from the lower dimensional objective formulation. The  
505 decision-makers can firstly analyze the performance of Pareto solutions in the sub-problem (*e.g.*,  
506 single or two-objective optimization) and then explore the tradeoff solutions using the previous  
507 analysis in the higher order objective space to satisfy the multi-stakeholders' benefits. Figs. 8a-  
508 8c illustrate the projection of four-objective Pareto solutions onto two-objective space with non-  
509 dominated front of the sub-problem constructed by the  $f_{TWS}$  and other objectives ( $f_{TCOST}$ ,  $f_{GSC}$  and  
510  $f_{SRI}$ ), respectively. As shown in Figs. 8a-8c, Solutions 1-3 are the compromise solutions in the  
511 Pareto front in the two-objective sub-problem which may be selected by decision-makers with  
512 no preference in the certain objectives. However, these high-performance solutions in the two-  
513 objective optimization exhibit worse performance in the other objective spaces. As illustrated in  
514 the plots (Fig. 8), Solutions 2 and 3 have higher  $f_{TCOST}$  than Solution 1 in Fig. 8a, Solutions 1 and  
515 3 have lower  $f_{GSC}$  than Solution 2 in Fig. 8b and Solutions 1 and 2 show lower  $f_{SRI}$  than Solution  
516 3 in Fig. 8c. Therefore, the decision-makers need identify the true compromise solution that  
517 performs well in the four objectives simultaneously. In this study, Solution 4 is closest to the  
518 corresponding objective values of the compromise solutions (Solutions 1-3) simultaneously and  
519 can be the true compromise solution in the 4-dimensional tradeoff surface. Additionally, Solution  
520 5 has the largest objective value of total water supply rate in the approximate Pareto front  
521 satisfying the constraints of maximum groundwater drawdown and minimum lake level. Solution  
522 6 corresponds to the compromise solution in the non-dominated front of  $f_{GSC}$  and  $f_{SRI}$ , which  
523 indicates the perfect performance in the protection of regional groundwater storage and water  
524 balance of the lake.



525  
 526 **Fig. 8.** Identification of six interesting solutions (Solutions 1-6) from the four-dimensional approximate Pareto  
 527 set and the green arrow is the preferred direction for each objective.

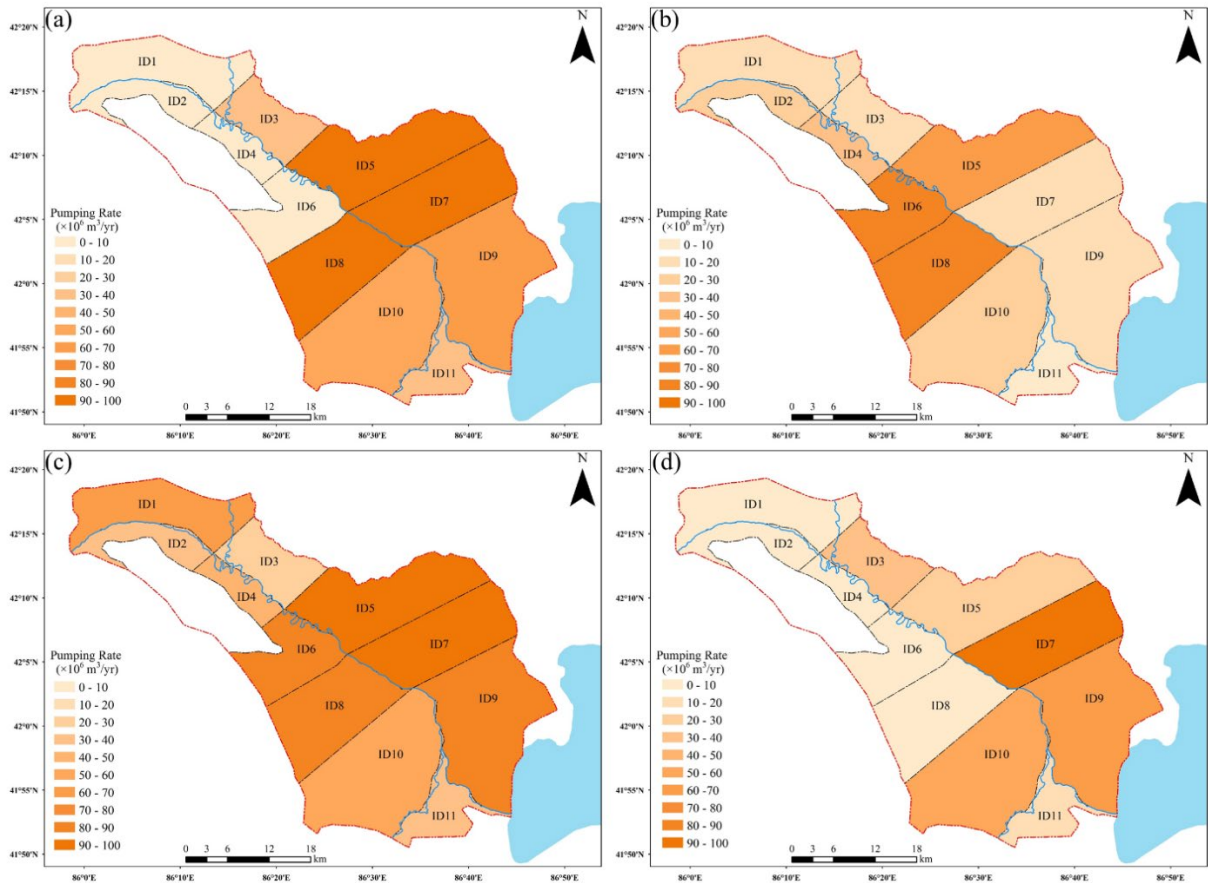
528 In this study, Solutions 4, 5 and 6 are selected to elucidate the variation of groundwater  
 529 abstraction and surface water diversion compared with the scheme before optimization (Solution  
 530 7). The objective values of selected solutions are listed in Table 2. It can be observed that Solution  
 531 4 can achieve similar total water supply rate while the cost of water delivery can reduce 34.4%  
 532 compared with Solution 7. The result shows that Solution 7 is sub-optimal from the aspect of  
 533 expenditure of water supply. Moreover, the surface runoff inflow to lake in Solution 4 achieves  
 534 the increment of 38.2 Mm<sup>3</sup>/yr and the depletion in groundwater storage obtains the reduction of  
 535 19.9 Mm<sup>3</sup>/yr. However,  $f_{GSC}$  of Solution 4 is still less than zero, which demonstrates the loss of  
 536 groundwater storage compared with initial state. Therefore, Solution 6 is a preferred water use  
 537 scheme from the aspects of maximization of groundwater storage and surface runoff inflow to  
 538 lake simultaneously. The objectives of Solution 6 in Table 2 show reducing 143.0 Mm<sup>3</sup>/yr of  $f_{TWS}$   
 539 in the scheme before optimization can achieve the increment of groundwater storage with 21.9

540 Mm<sup>3</sup>/yr and augment 63.0 Mm<sup>3</sup>/yr of surface runoff inflow to lake. Solution 5 represents the  
 541 potential of water resources exploitation in YB and can augment 26% of total water supply rate  
 542 compared with Solution 7. Interestingly, it can be found that, in Solutions 5 and 7, groundwater  
 543 storage depletion (83.9 Mm<sup>3</sup>/yr) is more rapid than the reduction of surface runoff inflow to the  
 544 lake (18.5 Mm<sup>3</sup>/yr). Hence, groundwater abstraction is probably preferred option to provide the  
 545 resiliency of water supply in the face of the increased water demands.

546 **Table 2.** The objective values corresponding to several solutions

Objective	Solution 4	Solution 5	Solution 6	Solution 7
$f_{TWS} (\times 10^8 \text{ m}^3/\text{yr})$	10.7406	12.7355	8.6712	10.1032
$f_{TCOST} (\times 10^6 \text{ CNY}/\text{yr})$	54.3013	92.1498	42.9522	82.7827
$f_{GSC} (\times 10^8 \text{ m}^3/\text{yr})$	-0.2471	-1.2856	0.2192	-0.4462
$f_{SRI} (\times 10^8 \text{ m}^3/\text{yr})$	17.5698	17.0030	17.8180	17.1880

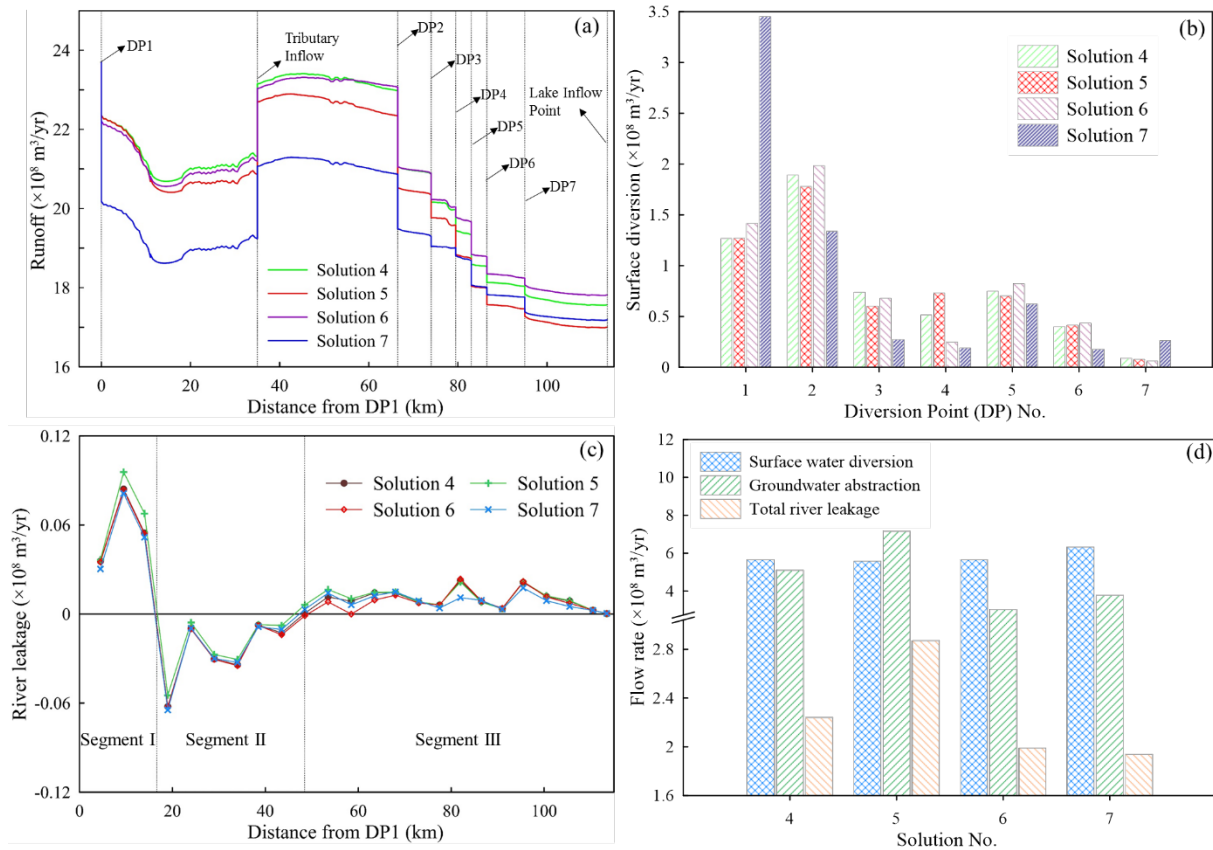
547 Fig. 9 illustrated the spatial distribution of the pumping rates of the selected solutions at 11  
 548 irrigation districts. As shown in Figs. 9a and 9b, Solution 4 shows groundwater abstraction in the  
 549 ID3, ID5 and ID7-ID11 can be increased in comparison to Solution 7. It can be noted that the  
 550 pumping rates in ID7 and ID9 can be largely elevated due to lower exploitation in the past and  
 551 shallow groundwater depth. The groundwater abstraction in ID1, ID2, ID4 and ID6 should be  
 552 reduced especially for the pumping rate in ID6 which exhibits abrupt decline. As shown in Fig.  
 553 9c, Solution 5 with the maximization of  $f_{TWS}$  demonstrates that a large amount of groundwater  
 554 can be abstracted in the ID5-ID9 (greater than 80.0 Mm<sup>3</sup>/yr) which implies water managers can  
 555 implement groundwater abstraction in those districts to satisfy the augmentation of water supply.  
 556 In Fig. 9d, Solution 6 is a desired scheme with the maximization of environment benefits in  
 557 groundwater storage and runoff recharge to the lake. The spatial differentiation of groundwater  
 558 abstraction in Solution 6 is similar with those in the 4-dimensional compromise solution  
 559 (Solution 4). However, in Solution 6, the pumping rates in the ID5 and ID8 show obvious decline,  
 560 which implies that water managers can lower the groundwater abstraction in these regions to  
 561 achieve more environment benefit in groundwater storage.



562  
 563 **Fig. 9.** The spatial distribution of the pumping rates in the 11 irrigation districts for the four selected schemes  
 564 of (a) Solution 4, (b) Solution 7, (c) Solution 5, and (d) Solution 6, respectively.

565 Fig. 10 illustrates the spatial patterns of surface water diversion along the mainstream of  
 566 Kaidu River. As show in Fig. 10a, seven diversion points (DP1-DP7) with the reduction of runoff  
 567 are clearly identified. The runoff at the 35 km from DP1 exhibits obvious rise due to the inflow  
 568 in the tributary. The river runoff at the lake inflow point is the surface runoff inflow to the lake  
 569 that is  $f_{SRI}$  objective. It can be observed that the surface runoff in the scheme before optimization  
 570 (Solution 7) in DP1 shows the abrupt decline than Pareto-optimal solutions (Solutions 4, 5 and  
 571 6) which responds to the distribution of surface diversion in Fig. 10b. Moreover, Solution 7 has  
 572 the lowest runoff between DP1 and DP4 even though exists slight increase in the lake inflow  
 573 point. Therefore, a significant increase of surface water diversion in DP1 controls the available  
 574 runoff in the downstream segments. The water managers should reduce the surface water  
 575 diversion in DP1 to ensure sufficient runoff in the lower reaches of Kaidu River for the

576 adjustment of multi-stakeholders' benefits. Solution 4 is a compromise scheme that exhibits  
577 lower runoff compared with Solution 6 from DP4 to the end of river, due to the larger water  
578 diversion in DP4, which triggers the reduction of surface runoff inflow to lake. Solution 5 is a  
579 potential of regional water resources exploitation in YB and has smaller available runoff than  
580 Solutions 4 and 6, approximating to more water diversion in Kaidu River. Fig. 10c further  
581 demonstrates the interaction of surface water and groundwater along the mainstream of the river.  
582 The upper segment (Segment I) is a losing segment that means surface water exchange from  
583 stream to aquifer and the middle segment (Segment II) is a gaining segment that indicates  
584 groundwater exchange from aquifer to stream. Then the lower segment (Segment III) turns into  
585 a losing segment. It can be noted that Segment I and Segment II have strong interaction between  
586 SW and GW whereas Segment III exhibits exchange with a lower leakage rate. As illustrated in  
587 Fig. 10d, the distribution of total river leakage shows that Solution 5 with the potential of water  
588 supply corresponds to the maximum river leakage caused by the maximum groundwater  
589 abstraction. The river leakage in Solutions 6 and 7 corresponds to lower groundwater abstraction.  
590 Consequently, groundwater abstraction is a dominated factor for the interaction of SW and GW  
591 in the basin. The river leakage in Solution 4 is clearly larger than Solution 7, which is seemingly  
592 undesired for water managers. However, augmenting groundwater abstraction ( $131.0 \text{ Mm}^3/\text{yr}$ )  
593 at the cost of river leakage ( $30.0 \text{ Mm}^3/\text{yr}$ ) can lower surface water diversion ( $67.0 \text{ Mm}^3/\text{yr}$ ) that  
594 is highly sensitive to the runoff inflow to Bosten Lake. Therefore, groundwater abstraction is  
595 probably a desired water use pattern in YB.



596  
 597 **Fig. 10.** Variation of surface runoff and river leakage along the stem stream of Kaidu River: (a) the profile of  
 598 river runoff; (b) the distribution of surface water diversion at the different diversion points; (c) the profile of  
 599 river leakage; (d) the components of total river leakage, groundwater abstraction and surface water diversion  
 600 for several typical Solutions 4-7.

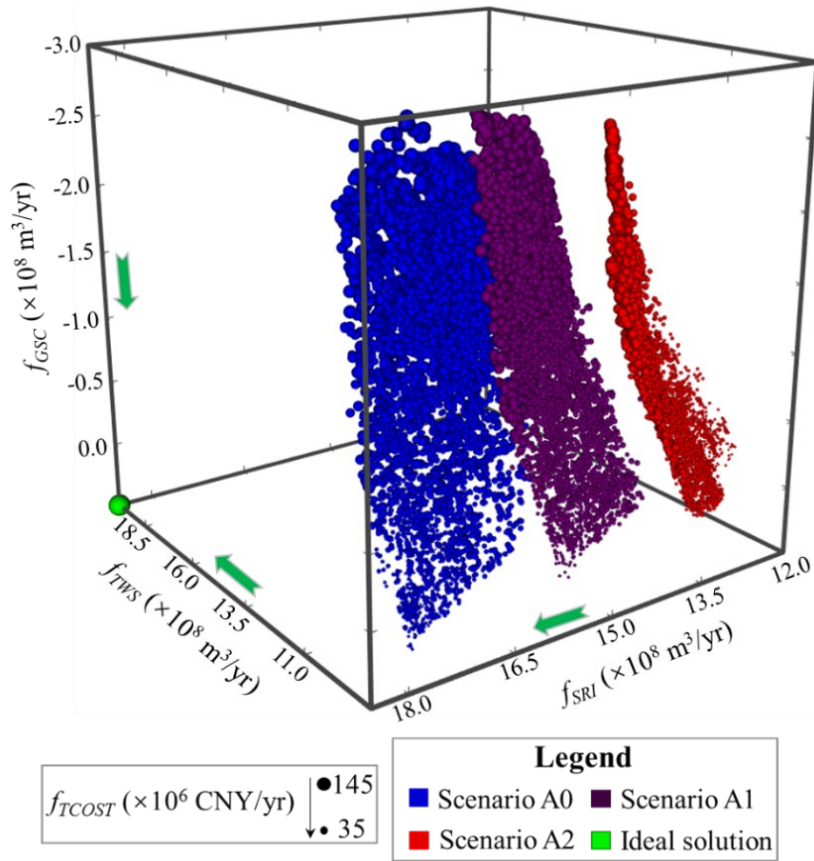
601 *4.3 Impacts of runoff change*

602 Kaidu River plays a crucial role to sustain regional water balance in YB and flows through  
 603 Dashankou station (Fig. 2) into the basin. The river supplies the majorities of surface water  
 604 diversion by an aqueduct system for agricultural irrigation and constitutes about 97% of total  
 605 annual inflow to Bosten Lake. The runoff in Kaidu River is mainly originated from mountainous  
 606 precipitation and melting glacier water in the Tianshan Mountains region. However, the  
 607 remarkable climate changes have caused a significant increase in both temperature and  
 608 precipitation over the past 50 years in Xinjiang (Li et al., 2013). The changing climate probably  
 609 increased the glacier melt and snowmelt in the upper part of Kaidu River and then caused the  
 610 growth of the river runoff between 1999 and 2002, with the highest runoff in 2002 of 5.7 billion

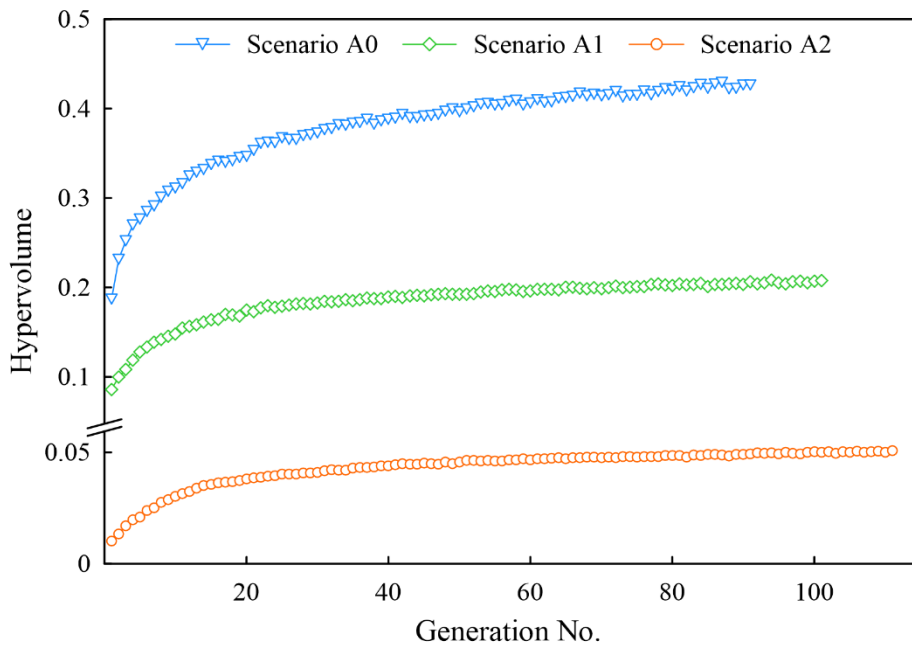
611 m<sup>3</sup>/year (Zhou et al., 2015). However, the long-term climate change may reduce runoff in Kaidu  
612 River attributing to the depletion of small or mid-size glaciers and snow line receding in the  
613 middle Tianshan Mountains region. Li et al. (2012) observed that surface area of snow in Kaidu  
614 River Basin reduced largely between 2000 and 2010. Therefore, it is essential to explore the  
615 impact of runoff reduction in Kaidu River on the regional water resources management for the  
616 local socioeconomic and environmental development.

617 The last part of our study implemented multi-objective optimization by resetting the runoff  
618 inflow at the first diversion point (DP1) in Kaidu River with the duplicated model parameters  
619 and the inputs of source and sink terms. Ba et al. (2018) employed the SWAT model with three  
620 RCMs (regional climate models) to analyze the influences of climate change on the streamflow  
621 in Dashankou station. The study results show that the annual streamflow will decrease during  
622 2020-2049 and reaches to the largest reduction percentage of 20.1% and 22.3% during 2040-  
623 2049 under RCP4.5 and RCP8.5 scenarios, respectively. We defined three runoff scenarios in  
624 relation to climate change in terms of the work of Ba et al. (2018), which are to maintain the  
625 current runoff (Scenario A0), reduce 10% of the runoff (Scenario A1) and reduce 20% of the  
626 runoff (Scenario A2), respectively. In the management model, the constraint of lake level is  
627 altered to the smaller value (1044.5m) and maximum groundwater drawdown is reset to 10m to  
628 avoid much more infeasible solutions in the population, which probably inhibits the convergence  
629 of the optimization. Fig. 11 shows all Pareto-optimal solutions in the four-dimensional objective  
630 space under the runoff scenarios. It is clearly observed that the tradeoff surface with current  
631 runoff (Scenario A0) is closest to the ideal solution and those with runoff reduction are farther  
632 from the solution. Scenario A2 based solutions exhibit worst performance owing to the greatest  
633 extent of runoff reduction. Moreover, we rescaled the objective range to the interval [0, 1] and  
634 set the reference point to the objective vector [1, 1, 1, 1] to calculate the HV metric of  
635 approximate Pareto solutions under the runoff scenarios. Fig. 12 shows the evolution of HV and

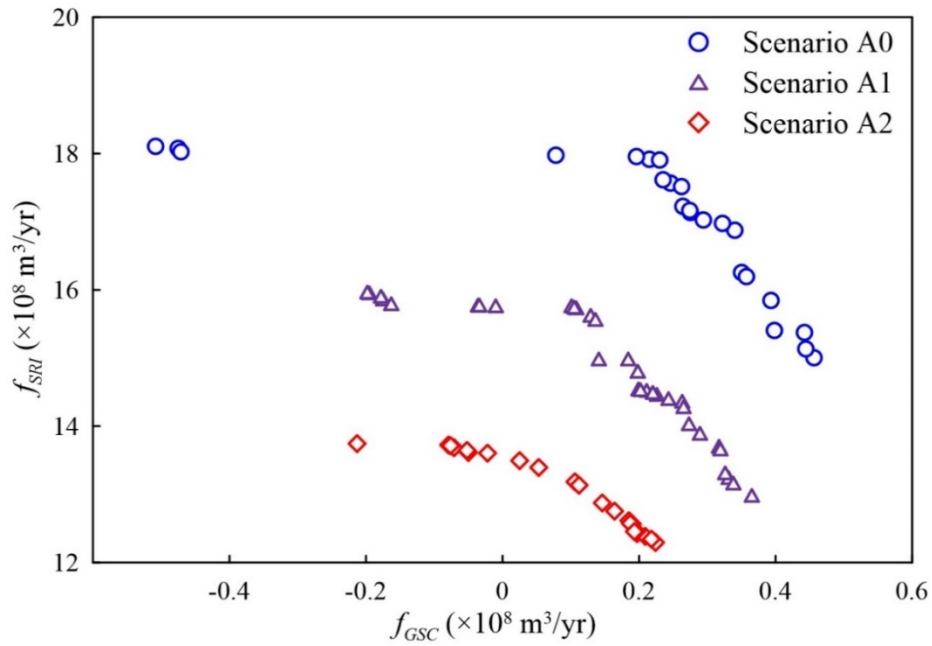
636 the number of generation. Judged from the performance evolution, tradeoff solutions under  
637 Scenario A0 achieve the largest HV and those in Scenario A2 have the lowest HV, which shows  
638 the solutions are far away from the ideal Pareto solution. Therefore, the exploitation extent of  
639 surface diversion and groundwater abstraction should be diminished in the face of runoff  
640 reduction in relation to climate change. In Fig. 11, the approximate Pareto solutions in Scenarios  
641 A0, A1 and A2 does not exists when  $f_{SRI}$  is greater than 1801.33  $Mm^3/yr$  in Scenario A0, 1596.33  
642  $Mm^3/yr$  in Scenario A1 and 1374.58  $Mm^3/yr$  in Scenario A2, which means the loss of diversity  
643 of Pareto solutions. The reason is that augmenting  $f_{TWS}$  causes more decline of  $f_{SRI}$  and the lake  
644 level compared with no reduction in runoff in Scenario A0, which probably generates a large  
645 amount of unfeasible solutions violating the constraint of minimum lake level. The finding also  
646 shows that runoff in Kaidu River through YB is a dominant factor controlling the variation of  
647 lake level. To investigate the effect of runoff reduction on the environmental benefits, Fig. 13  
648 shows the non-dominated fronts in the  $f_{GSC}$  and  $f_{SRI}$  objectives space across Scenarios A0, A1 and  
649 A2. The solutions in Scenario A2 are completely dominated by the solutions in Scenarios A0 and  
650 A1. The solutions in Scenario A0 show the best Pareto optimality. Therefore, the runoff reduction  
651 results in obvious loss of environmental benefits. It is noteworthy that  $f_{SRI}$  with Scenarios A1 and  
652 A2 will be reduced under the similar  $f_{GSC}$ . In the optimization, in order to maximize irrigation  
653 water supply, sustaining similar groundwater storage in Scenarios A1 and A2 has to be at the cost  
654 of river runoff decline to increase surface water diversion. Hence, it is essential for water  
655 managers to realize the conflict of conjunctive use of SW and GW for water resources  
656 management in arid inland basin.



657  
 658 **Fig. 11.** The tradeoff solutions under Scenarios A0 (maintain current runoff), A1 (reduce the runoff by 10%)  
 659 and A2 (reduce the runoff by 20%), and the sphere size indicates the value of  $f_{TCOST}$ . The green arrow is the  
 660 direction of better performance for each objective.



661  
 662 **Fig. 12.** Evolution of the hypervolume metric over the generation number for Scenarios A0, A1 and A2.



663

664 **Fig. 13.** Non-dominated fronts of Scenarios A0, A1 and A2 between objectives of  $f_{GSC}$  vs.  $f_{SRI}$ .

665 **5. Conclusions**

666 The study proposed a multi-objective optimization framework for the integrated surface  
 667 water and groundwater management and demonstrated its effectiveness through a spatial  
 668 optimization of water use practices for agricultural irrigation in YB, a typical arid inland basin  
 669 in northwest China. The well-calibrated simulation model with MODFLOW-NWT was  
 670 developed to model the interaction of surface water (*i.e.*, Kaidu River and Bosten Lake) and  
 671 groundwater. Then this study presented a new MOEA (the epsilon multi-objective memetic  
 672 algorithm,  $\epsilon$ -MOMA) and linked it with the numerical model to solve the multi-objective  
 673 management model. The optimization model is composed of the four conflicting objectives:  
 674 maximizing total water supply rate, minimizing total cost of transporting water from water intake  
 675 points to water use destinations, maximizing the groundwater storage in the aquifer and  
 676 maximizing the surface runoff inflow from Kaidu River to Bosten Lake. An interactive  
 677 visualization tool was applied to explore 4-dimensional tradeoff surface in a global view. Results  
 678 showed augmenting water supply caused the larger cost of water delivery, reduced the runoff  
 679 inflow to lake and aggravated the loss of groundwater storage. The 2-dimensional compromise

680 schemes selected from the non-dominated fronts between  $f_{TWS}$  and other objectives exhibited  
681 significant decision bias in the higher order objective spaces. Therefore, it is crucial for water  
682 managers to explore water management schemes in the multi-objective tradeoff surface.

683 The 4-dimensional compromise solution is obtained to investigate performance of existing  
684 scheme. Result shows that the water use practices before optimization have to be regulated to  
685 avoid unnecessary capital expenditure of transporting water. However, the compromised solution  
686 indicates groundwater storage is still decreasing. Thus, water managers may be inclined to adopt  
687 the Pareto-optimal scheme satisfying minimum water demands to prevent the loss of  
688 groundwater storage and runoff inflow to the lake. In the practical application, water managers  
689 should identify specific irrigation water demands and environmental constraints to discover  
690 preferred water use schemes. Moreover, the regulation of groundwater abstraction is more  
691 flexible than surface water diversion in the Pareto-optimal solutions, which is an important  
692 implication for the resiliency of water resources management. The water use schemes are subject  
693 to the spatial complexity of strong SW-GW interaction. That is to say, the integrated management  
694 of SW-GW is highly desired to reflect the complex interactions of water resources system in the  
695 optimization. The scenarios of runoff change were then generated to investigate the effect of  
696 runoff depletion in Kaidu River on the regional water resources management. The findings  
697 showed that reducing runoff inflow to the basin could lead to the degradation of Pareto solutions  
698 compared with those based on the current runoff scenario. In this light, it is crucial to implement  
699 stricter water resources management and explore potential water-saving strategies under the  
700 future conditions.

701 The findings are applicable to regional water resources management in other typical arid  
702 inland basins with complex groundwater-river-lake interactions and intensive agricultural  
703 development. Due to the data-scarcity in the basin-scale full-coupled modeling and limitations  
704 of simulation model, the predictive uncertainty is inevitable. However, the simulation model can

705 reflect the responses of water resources system to the conjunctive use of SW and GW for  
706 agricultural irrigation. The parameter uncertainty can be addressed with the construction of  
707 adequate monitoring system for modeling in the future work. Meanwhile, future research should  
708 focus on exploiting fully coupled simulation model to accurately model basin-scale water  
709 resources system and avoid decision bias derived from the limitations of model. Moreover, the  
710 deep uncertainty showing the lack of consensus on their underlying probability distribution and  
711 consequences (*e.g.*, land use change, climate change) is a key factor to affect the robustness and  
712 reliability of the optimal solutions under the changing world. In the simulation-optimization  
713 framework, integrating these factors into the management model to explore optimal schemes is  
714 a research focus in the future.

#### 715 **Code and data availability**

716 The data used in this study are provided on request by the Xinjiang Tarim River Basin Authority  
717 in China and are not publicly accessible. The detailed data information can be found in Table S2  
718 in the supplementary material. The codes can be provided through direct request to the  
719 corresponding author.

#### 720 **Supplement**

721 The supplement related to this article is available on the uploaded file (Supplement\_to\_HESS-  
722 2019-278.pdf).

#### 723 **Author contribution**

724 JS, YY, JFW and JCW conceptualized the paper and its scope. XMS, JL and MW collected the  
725 data. JS implemented the simulation model with some contributions from MW. JS developed the  
726 code, performed the study, and wrote the initial manuscript. JS, YY and JFW revised the paper.  
727 All authors contributed to the manuscript preparation.

728 **Competing interests**

729 The authors declare that they have no conflict of interest.

730 **Acknowledgements**

731 This study is jointly supported by the National Natural Science Foundation of China (41730856  
732 and 41772254) and the National Key Research and Development Plan of China  
733 (2016YFC0402800). The numerical calculations in this study have been implemented on the  
734 IBM Blade cluster system in the High Performance Computing Center of Nanjing University,  
735 China. In particular, the authors are grateful to Referee Dr. Joseph Kasprzyk of the University of  
736 Colorado at Boulder, Referee Dr. Qiankun Luo of the Hefei University of Technology and an  
737 anonymous referee for their insightful comments and invaluable suggestions on the manuscript.

738 **Financial support**

739 This research has been supported by the National Natural Science Foundation of China  
740 (41730856 and 41772254) and the National Key Research and Development Plan of China  
741 (2016YFC0402800).

742 **Review statement**

743 This paper was edited by Dimitri Solomatine and reviewed by Joseph Kasprzyk and one  
744 anonymous referee.

745 **References**

- 746 Bader, J. and Zitzler, E.: HypE: an algorithm for fast hypervolume-based many-objective  
747 optimization, *Evol. Comput*, 19(1), 45-76, [doi:10.1162/EVCO\\_a\\_00009](https://doi.org/10.1162/EVCO_a_00009), 2011.
- 748 Ba, W., Du, P., Liu, T., Bao, A., Luo, M., Mujtaba, H., and Qin, C.: Simulating hydrological  
749 responses to climate change using dynamic and statistical downscaling methods: a case  
750 study in the Kaidu River Basin, Xinjiang, China. *J. Arid Land*, 10(6): 905-920,

751           doi:10.1007/s40333-018-0068-0, 2018.

752 Beh, E.H., Zheng, F., Dandy, G.C., Maier, H.R., and Kapelan, Z.: Robust optimization of water  
753           infrastructure planning under deep uncertainty using metamodels, *Environ. Model. Softw.*,  
754           93, 92-105, [doi:10.1016/j.envsoft.2017.03.013](https://doi.org/10.1016/j.envsoft.2017.03.013), 2017.

755 Chen, B., Zeng, W.H., Lin, Y.B., and Zhang, D.F.: A new local search-based multiobjective  
756           optimization algorithm, *IEEE Trans.*, 19(1), 50-73, [doi:10.1109/TEVC.2014.2301794](https://doi.org/10.1109/TEVC.2014.2301794),  
757           2015.

758 Chen, Y., Chen, Y., Xu, C., Ye, Z., Li, Z., Zhu, C., and Ma, X.: Effects of ecological water  
759           conveyance on groundwater dynamics and riparian vegetation in the lower reaches of  
760           Tarim River, China, *Hydrol. Process.*, 24, 170-177, [doi:10.1002/hyp.7429](https://doi.org/10.1002/hyp.7429), 2010.

761 Deb, K. and Agrawal, R.B.: Simulated binary crossover for continuous search space, Indian  
762           Institute of Technology, Kanpur, UP, India, Tech. Rep. IITK/ME/SMD-94027, Nov. 1994.

763 Deb, K., Joshi, D., and Anand, A.: Real-coded evolutionary algorithms with parent-centric  
764           recombination, *Computation Intelligence, Proceedings of the World on Congress on*, 1, 61-  
765           66, 2002a.

766 Deb, K., Pratap, A., Agarwal, S., and Meyarivan, T.: A fast and elitist multi-objective genetic  
767           algorithm: NSGA-II, *IEEE Trans.*, 6(2), 182-197, [doi:10.1109/4235.996017](https://doi.org/10.1109/4235.996017), 2002b.

768 Deb, K., Thiele, L., Laumanns, M., and Zitzler, E.: Scalable multi-objective optimization test  
769           problems, in: *proceeding of the congress on evolutionary computation (CEC-2002)*, 825-  
770           830, 2002c.

771 Deep, K. and Thakur, M.: A new crossover operator for real coded genetic algorithms, *Appl.*  
772           *Math. Comput.*, 188, 895-911, [doi:10.1016/j.amc.2006.10.047](https://doi.org/10.1016/j.amc.2006.10.047), 2007.

773 Eker, S. and Kwakkel, J.H.: Including robustness considerations in the search phase of Many-  
774           Objective Robust Decision Making, *Environ. Model. Softw.*, 105, 201-216,  
775           [doi:10.1016/j.envsoft.2018.03.029](https://doi.org/10.1016/j.envsoft.2018.03.029), 2018.

776 Fleming, P., Purshouse, R., and Lygoe, R.: Many-objective optimization: an engineering design  
777 perspective. In: Coello Coello, C., Hernández Aguirre, A., Zitzler, E. (Eds.), Evolutionary  
778 Multi-Criterion Optimization. Lecture Notes in Computer Science. Springer, Berlin  
779 Heidelberg, 14-32, 2005.

780 Gao, H. and Yao, Y.: Quantitative effect of human activities on water level change of Bosten  
781 Lake in recent 50 years, *Scientia Geographica Sinica*, 25, 3305-3309, 2005 (in Chinese  
782 with English abstract).

783 Hadka, D., Herman, J., Reed, P., and Keller, K.: An open source framework for many objective  
784 robust decision making, *Environ. Model. Softw.*, 74, 114-129,  
785 [doi:10.1016/j.envsoft.2015.07.014](https://doi.org/10.1016/j.envsoft.2015.07.014), 2015.

786 Hadka, D. and Reed, P.M.: Borg: an auto-adaptive many-objective framework, *Evol. Comput*,  
787 21(2), 213-259, [doi:10.1162/EVCO\\_a\\_00075](https://doi.org/10.1162/EVCO_a_00075), 2013.

788 Hao, X. and Li, W.: Impacts of ecological water conveyance on groundwater dynamics and  
789 vegetation recovery in the lower reaches of the Tarim River in northwest China, *Environ.*  
790 *Monit. Assess.*, 186(11), 7605-7616, [doi:10.1007/s10661-014-3952-x](https://doi.org/10.1007/s10661-014-3952-x), 2014.

791 Harbaugh, A.W.: MODFLOW-2005, the U.S. Geological Survey modular ground-water model -  
792 the Ground-Water Flow Process: U.S. Geological Survey Techniques and Methods 6-A16,  
793 2005.

794 Hassanzadeh, E., Elshorbagy, A., Wheater, H., and Gober, P.: Managing water in complex  
795 systems: An integrated water resources model for Saskatchewan, Canada, *Environ. Model.*  
796 *Softw.*, 58, 12-26, [doi:10.1016/j.envsoft.2014.03.015](https://doi.org/10.1016/j.envsoft.2014.03.015), 2014.

797 Hu, L.T., Chen, C.X., Jiao, J.J., and Wang, Z.J.: Simulated groundwater interaction with rivers  
798 and springs in the Heihe river basin, *Hydrol. Process.*, 21(20), 2794-2806,  
799 [doi:10.1002/hyp.6497](https://doi.org/10.1002/hyp.6497), 2007.

800 Inselberg, A.: *Parallel Coordinates: Visual Multidimensional Geometry and Its Applications*,

801 Springer, New York, USA, [doi:10.1007/978-0-387-68628-8](https://doi.org/10.1007/978-0-387-68628-8), 2009.

802 Kasprzyk, J.R., Reed, P.M., Characklis, G.W., and Kirsch, B.R.: Many-objective *de Novo* water  
803 supply portfolio planning under deep uncertainty, *Environ. Model. Softw.*, 34, 87-104,  
804 [doi:10.1016/j.envsoft.2011.04.003](https://doi.org/10.1016/j.envsoft.2011.04.003), 2012.

805 Kasprzyk, J.R., Reed, P.M., and Hadka, D.M.: Battling arrow's paradox to discover robust water  
806 management alternatives, *J. Water Resour. Plan. Manag.*, 142(2), 04015053,  
807 [doi:10.1061/\(ASCE\)WR.1943-5452.0000572](https://doi.org/10.1061/(ASCE)WR.1943-5452.0000572), 2015.

808 Khare, D., Jat, M.K., and Ediwahyunan.: Assessment of conjunctive use planning options: a  
809 case study of Sapon irrigation command area of Indonesia, *J. Hydrol.*, 328(3-4), 764-777,  
810 [doi:10.1016/j.jhydrol.2006.01.018](https://doi.org/10.1016/j.jhydrol.2006.01.018), 2006.

811 Kollat, J.B. and Reed, P.: A framework for visually interactive decision-making and design using  
812 evolutionary multi-objective optimization (VIDEO), *Environ. Model. Softw.*, 22 (12),  
813 1691-1704, [doi:10.1016/j.envsoft.2007.02.001](https://doi.org/10.1016/j.envsoft.2007.02.001), 2007.

814 Laumanns, M., Thiele, L., Deb, K., and Zitzler, E.: Combining convergence and diversity in  
815 evolutionary multi-objective optimization, *Evol. Comput.*, 10(3), 263-282,  
816 [doi:10.1162/106365602760234108](https://doi.org/10.1162/106365602760234108), 2002.

817 Li, B., Chen, Y., Shi, X., Chen, Z., and Li, W.: Temperature and precipitation changes in different  
818 environments in the arid region of northwest China, *Theor. Appl. Climatol.*, 112, 589-596,  
819 [doi:10.1007/s00704-012-0753-4](https://doi.org/10.1007/s00704-012-0753-4), 2013.

820 Li, Q., Li, L.H., and Bao, A.M.: Snow cover change and impact on streamflow in the Kaidu  
821 River Basin, *Resources Science*, 34, 91-97, 2012 (in Chinese with English abstract).

822 Liu, L., Luo, Y., He, C., Lai, J., and Li, X.: Roles of the combined irrigation, drainage, and storage  
823 of the canal network in improving water reuse in the irrigation districts along the lower  
824 Yellow River, China, *J. Hydrol.*, 391(1-2), 157-174, [doi:10.1016/j.jhydrol.2010.07.015](https://doi.org/10.1016/j.jhydrol.2010.07.015),  
825 2010.

826 Liu, L., Zhao, J., Zhang, J., Peng, W., Fan, J., and Zhang, T.: Water balance of Lake Bosten using  
827 annual water-budget method for the past 50 years, *Arid Land Geography*, 36, 33-40, 2013  
828 (in Chinese with English abstract).

829 Maier, H.R., Guillaume, J.H.A., van Delden, H., Riddell, G.A., Haasnoot, M., and Kwakkel, J.H.:  
830 An uncertain future, deep uncertainty, scenarios, robustness and adaptation: How do they  
831 fit together? *Environ. Model. Softw.*, 81, 154-164, [doi: 10.1016/j.envsoft.2016.03.014](https://doi.org/10.1016/j.envsoft.2016.03.014),  
832 2016.

833 Maier, H.R., Kapelan, Z., Kasprzyk, J., Kollat, J., Matott, L.S., Cunha, M.C., Dandy, G.C., Gibbs,  
834 M.S., Keedwell, E., Marchi, A., Ostfeld, A., Savic, D., Solomatine, D.P., Vrugt, J.A.,  
835 Zecchin, A.C., Minsker, B.S., Barbour, E.J., Kuczera, G., Pasha, F., Castelletti, A., Giuliani,  
836 M., and Reed, P.M.: Evolutionary algorithms and other metaheuristics in water resources:  
837 current status, research challenges and future directions, *Environ. Model. Softw.*, 62, 271-  
838 299, [doi:10.1016/j.envsoft.2014.09.013](https://doi.org/10.1016/j.envsoft.2014.09.013), 2014.

839 Maier, H.R., Razavi, S., Kapelan, Z., Matott, L.S., Kasprzyk, J., and Tolson, B.A.: Introductory  
840 overview: Optimization using evolutionary algorithms and other metaheuristics, *Environ.*  
841 *Model. Softw.*, 114, 195-213. [doi:10.1016/j.envsoft.2018.11.018](https://doi.org/10.1016/j.envsoft.2018.11.018), 2019.

842 Mamat, Z., Yimit, H., Ji, R.Z.A., and Eziz, M.: Source identification and hazardous risk  
843 delineation of heavy metal contamination in Yanqi basin, northwest China, *Sci. Total*  
844 *Environ.*, 493, 1098-1111, [doi:10.1016/j.scitotenv.2014.03.087](https://doi.org/10.1016/j.scitotenv.2014.03.087), 2014.

845 Matteo, M.D., Maier, H.R., and Dandy, G.C.: Many-objective portfolio optimization approach  
846 for stormwater management project selection encouraging decision maker buy-in, *Environ.*  
847 *Model. Softw.*, 111, 340-355, [doi:10.1016/j.envsoft.2018.09.008](https://doi.org/10.1016/j.envsoft.2018.09.008), 2019.

848 McPhee, J. and Yeh, W.W.G.: Multiobjective optimization for sustainable groundwater  
849 management in semiarid regions, *J. Water Resour. Plan. Manag.*, 130(6), 490-497,  
850 [doi:10.1061/\(ASCE\)0733-9496\(2004\)130:6\(490\)](https://doi.org/10.1061/(ASCE)0733-9496(2004)130:6(490)), 2004.

851 Michael, L.M. and Leonard, F.K.: Documentation of a Computer Program to Simulate Lake-  
852 aquifer Interaction Using the Modflow Ground-water Flow Model and the Moc3d Solute-  
853 transport Model, U.S. Geological Water-Resources Investigations Report, 2000.

854 Niswonger, R.G., Panday, S., and Ibaraki, M.: MODFLOW-NWT, A Newton formulation for  
855 MODFLOW-2005: US Geological Survey Techniques and Methods 6-A37, 44 p, 2011.

856 Parsapour-Moghaddam, P., Abed-Elmdoust, A., and Kerachian, R.: A heuristic evolutionary  
857 game theoretic methodology for conjunctive use of surface and groundwater resources,  
858 Water Resour. Manag., 29(11), 3905-3918, [doi:10.1007/s11269-015-1035-6](https://doi.org/10.1007/s11269-015-1035-6), 2015.

859 Purshouse, R.C. and Fleming, P.J.: On the evolutionary optimization of many conflicting  
860 objectives, IEEE Trans., 11(6), 770-784, [doi:10.1109/TEVC.2007.910138](https://doi.org/10.1109/TEVC.2007.910138), 2007.

861 Reed, P.M., Hadka, D., Herman, J.D., Kasprzyk, J.R., and Kollat, J.B.: Evolutionary  
862 multiobjective optimization in water resources: The past, present and future, Adv Water  
863 Resour., 51, 438-456, [doi:10.1016/j.advwatres.2012.01.005](https://doi.org/10.1016/j.advwatres.2012.01.005), 2013.

864 Richard, G.N. and David, E.P.: Documentation of the Streamflow-Routing (SFR2) Package to  
865 Include Unsaturated Flow Beneath Streams-A Modification to SFR1, U.S. Geological  
866 Survey Techniques and Methods, pp. 6-A13, 2010.

867 Rothman, D. and Mays, L.W.: Water resources sustainability: development of a multi-objective  
868 optimization model, J. Water Resour. Plan. Manag., 140(12), 04014039,  
869 [doi:10.1061/\(ASCE\)WR.1943-5452.0000425](https://doi.org/10.1061/(ASCE)WR.1943-5452.0000425), 2013.

870 Safavi, H.R. and Esmikhani, M.: Conjunctive use of surface water and groundwater: application  
871 of support vector machines (SVMs) and genetic algorithms, Water Resour. Manag., 27(7),  
872 2623-2644, [doi:10.1007/s11269-013-0307-2](https://doi.org/10.1007/s11269-013-0307-2), 2013.

873 Sindhya, K., Deb, K., and Miettinen, K.: Improving convergence of evolutionary multiobjective  
874 optimization with local search: a concurrent-hybrid algorithm, Nat. Comput., 10(4), 1407-  
875 1430, [doi:10.1007/s11047-011-9250-4](https://doi.org/10.1007/s11047-011-9250-4), 2011.

876 Sindhya, K., Miettinen, K., and Deb, K.: A hybrid framework for evolutionary multiobjective  
877 optimization. *IEEE Trans.*, 17(4), 495-511, [doi:10.1109/TEVC.2012.2204403](https://doi.org/10.1109/TEVC.2012.2204403), 2013.

878 Singh, A.: Simulation-optimization modeling for conjunctive water use management, *Agric.*  
879 *Water Manag.*, 141, 23-29, [doi:10.1016/j.agwat.2014.04.003](https://doi.org/10.1016/j.agwat.2014.04.003), 2014.

880 Singh, A. and Panda, S.N.: Optimization and simulation modelling for managing the problems  
881 of water resources, *Water Resour. Manag.*, 27(9), 3421-3431, [doi:10.1007/s11269-013-0355-7](https://doi.org/10.1007/s11269-013-0355-7), 2013.

882

883 Storn, R. and Price, K.: Differential evolution - a simple and efficient heuristic for global  
884 optimization over continuous spaces, *J. Global Optim.*, 11(4), 341-359,  
885 [doi:10.1023/A:1008202821328](https://doi.org/10.1023/A:1008202821328), 1997.

886 Tian, Y., Zheng, Y., Wu, B., Wu, X., Liu, J., and Zheng, C.: Modeling surface water-groundwater  
887 interaction in arid and semi-arid regions with intensive agriculture, *Environ. Model. Softw.*,  
888 63, 170-184, [doi:10.1016/j.envsoft.2014.10.011](https://doi.org/10.1016/j.envsoft.2014.10.011), 2015.

889 Tsutsui, S., Yamamura, M., and Higuchi, T.: Multi-parent recombination with simplex crossover  
890 in real coded genetic algorithms, in *Genetic and Evolutionary Computation Conference*  
891 *(GECCO 1999)*, 1999.

892 Wang, W., Wang, X., Jiang, F., and Peng, D.: Response of runoff volume to climate change in  
893 the Kaidu River Basin in recent 30 years, *Arid Zone research*, 30, 743-748, 2013 (in  
894 Chinese with English abstract).

895 Wang, Y., Chen, Y., and Li, W.: Temporal and spatial variation of water stable isotopes ( $^{18}\text{O}$  and  
896  $^2\text{H}$ ) in the Kaidu River basin, Northwest China, *Hydrol. Process.*, 28(3), 653-661,  
897 [doi:10.1002/hyp.9622](https://doi.org/10.1002/hyp.9622), 2014.

898 Wichelns, D. and Oster, J.D.: Sustainable irrigation is necessary and achievable, but direct costs  
899 and environmental impacts can be substantial, *Agric. Water Manag.*, 86(1-2), 114-127,  
900 [doi:10.1016/j.agwat.2006.07.014](https://doi.org/10.1016/j.agwat.2006.07.014), 2006.

- 901 Woodruff, M.J., Reed, P.M., and Simpson, T.W.: Many objective visual analytics: rethinking the  
902 design of complex engineered systems, *Struct. Multidisc. Optim.*, 48(1), 201-219,  
903 [doi:10.1007/s00158-013-0891-z](https://doi.org/10.1007/s00158-013-0891-z), 2013.
- 904 Wu, B., Zheng, Y., Tian, Y., Wu, X., Yao, Y., Han, F., Liu, J., and Zheng, C.: Systematic  
905 assessment of the uncertainty in integrated surface water-groundwater modeling based on  
906 the probabilistic collocation method, *Water Resour. Res.*, 50, 5848-5865,  
907 [doi:10.1002/2014WR015366](https://doi.org/10.1002/2014WR015366), 2014.
- 908 Wu, B., Zheng, Y., Wu, X., Tian, Y., Han, F., Liu, J., and Zheng, C.: Optimizing water resources  
909 management in large river basins with integrated surface water-groundwater modeling: A  
910 surrogate-based approach, *Water Resour. Res.*, 51, 2153-2173,  
911 [doi:10.1002/2014WR016653](https://doi.org/10.1002/2014WR016653), 2015.
- 912 Wu, M., Wu, J., Lin, J., Zhu, X., Wu, J., and Hu, B.X.: Evaluating the interactions between  
913 surface water and groundwater in the arid mid-eastern Yanqi Basin, northwest China,  
914 *Hydrolog. Sci. J.*, 63(9), 1313-1331, [doi:10.1080/02626667.2018.1500744](https://doi.org/10.1080/02626667.2018.1500744), 2018.
- 915 Wu, X., Zheng, Y., Wu, B., Tian, Y., Han, F., and Zheng, C.M.: Optimizing conjunctive use of  
916 surface water and groundwater for irrigation to address human-nature water conflicts: A  
917 surrogate modeling approach, *Agric. Water Manag.*, 163, 380-392,  
918 [doi:10.1016/j.agwat.2015.08.022](https://doi.org/10.1016/j.agwat.2015.08.022), 2016.
- 919 Xiao, M., Wu F., Liao, H., Li, W., Lee, X., and Huang, R.: Characteristics and distribution of low  
920 molecular weight organic acids in the sediment porewaters in Bosten Lake, China, *J.*  
921 *Environ. Sci.*, 22(3), 328-337, [doi:10.1016/S1001-0742\(09\)60112-1](https://doi.org/10.1016/S1001-0742(09)60112-1), 2010.
- 922 Xu, H., Ye, M., Song, Y., and Chen, Y.: The natural vegetation responses to the groundwater  
923 change resulting from ecological water conveyances to the lower Tarim River, *Environ.*  
924 *Monit. Assess.*, 131(1-3), 37-48, [doi:10.1007/s10661-006-9455-7](https://doi.org/10.1007/s10661-006-9455-7), 2007.
- 925 Xu, J., Chen, Y., Bai, L., and Xu, Y.: A hybrid model to simulate the annual runoff of the Kaidu

926 River in northwest China, *Hydrol. Earth Syst. Sci.*, 20, 1447-1457, [doi:10.5194/hess-20-](https://doi.org/10.5194/hess-20-1447-2016)  
927 [1447-2016](https://doi.org/10.5194/hess-20-1447-2016), 2016.

928 Yang, C.C., Chang, L.C., Chen, C.S., and Yeh, M.S.: Multi-objective planning for conjunctive  
929 use of surface and subsurface water using genetic algorithm and dynamics programming.  
930 *Water Resour. Manag.*, 23(3), 416-437, [doi:10.1007/s11269-008-9281-5](https://doi.org/10.1007/s11269-008-9281-5), 2009.

931 Yao, J., Chen, Y., Zhao, Y., and Yu, X.: Hydro climatic changes of Lake Bosten in Northwest  
932 China during the last decades, *Sci Rep.*, 8, 9118, [doi:10.1038/s41598-018-27466-2](https://doi.org/10.1038/s41598-018-27466-2), 2018.

933 Yao, Y., Zheng, C., Liu, J., Cao, G., Xiao, H., Li, H., and Li, W.: Conceptual and numerical  
934 models for groundwater flow in an arid inland river basin, *Hydrol. Process.*, 29, 1480-1492,  
935 [doi:10.1002/hyp.10276](https://doi.org/10.1002/hyp.10276), 2015.

936 Zhang, Z., Hu, H., Tian, F., Yao, X., and Sivapalan, M.: Groundwater dynamics under water-  
937 saving irrigation and implications for sustainable water management in an oasis: Tarim  
938 River basin of western China, *Hydrol. Earth Syst. Sci.*, 18, 3951-3967, [doi:10.5194/hess-](https://doi.org/10.5194/hess-18-3951-2014)  
939 [18-3951-2014](https://doi.org/10.5194/hess-18-3951-2014), 2014.

940 Zheng, F., Zecchin, A.C., Maier, H.R., and Simpson, A.R.: Comparison of the searching behavior  
941 of NSGA-II, SAMODE, and Borg MOEAs applied to water distribution system design  
942 problems, *J. Water Resour. Plann. Manage.*, 142(7), 04016017,  
943 [doi:10.1061/\(ASCE\)WR.1943-5452.0000650](https://doi.org/10.1061/(ASCE)WR.1943-5452.0000650), 2016.

944 Zhou, H., Cheng, Y., Perry, L., and Li, W.: Implications of climate change for water management  
945 of an arid inland lake in Northwest China, *Lake Reserv Manage.*, 31(3), 202-213,  
946 [doi:10.1080/10402381.2015.1062834](https://doi.org/10.1080/10402381.2015.1062834), 2015.

947 Zizler, E., Thiele, L., Laumanns, M., Fonseca, C., da Fonseca, V.: Performance assessment of  
948 multiobjective optimizers: an analysis and review. *IEEE Trans.*, 7(2), 117-132,  
949 [doi:10.1109/TEVC.2003.810758](https://doi.org/10.1109/TEVC.2003.810758), 2003.